acta
geologica
polonica

Vol. 45, No. 1-2 Warszawa 1995

ELŻBIETA DUBIŃSKA, JACEK JELITTO & ANDRZEJ KOZŁOWSKI

Origin and evolution of the granite/serpentinite reaction zones at Wiry, Lower Silesia

ABSTRACT: Contact schists between Variscan hybridal granitoid apophyses and older serpentinite at Wiry, Lower Silesia, are composed of phlogopite and chlorite, and their alteration products (vermiculite, smectite, regularly interstratified mica/vermiculite, various interstratified chlorite/vermiculite and chlorite/smectite with asymmetric iron location, and three-component interstratified mica/vermiculite/chlorite), as recognized by means of *XRD* examination and computer simulations. The peak contact metamorphism yielded disseminated tremolite-to-pargasite amphiboles, and minor apatite. Its conditons, determined from aluminium content and fluid inclusions in hornblende, achieved 2.6 Kbar and 560°C. The parent solutions had Ca-Na-Cl composition of variable calcium and sodium proportions; the variations were related to albitization of the adjacent Strzegom granitoids. The layer silicates assemblage may be considered as an equivalent of a predecessor of weathering silicate nikiel ores from the worldwide-known deposit at the neighboring ultrabasic massif of Szklary.

INTRODUCTION

The magnesite mine of Wiry is located in Lower Silesia, southwest of Wrocław, in the western part of the Jordanów-Gogołów serpentinite massif (Text-fig. 1), close to the Variscan granitoid massif of Strzegom (*c.* 280 Ma; *see* PIN & *al.* 1989).

The purpose of this study is to elaborate a model of the origin of the contact zones from Wiry, to explain their relation to the Strzegom granitoid massif and the Jordanów-Gogołów serpentinites, and to discuss briefly their place in a complex geologic history of the area.

The contact zones between leucocratic and ultrabasic rocks have attracted the interest of geologists for many years, both between older granite and younger ultrabasic rock and, on the other hand, between younger granite and older ultrabasic rock (*e.g.* BASSET 1963, TROMMSDORFF & EVANS 1972, SANFORD 1982, MATTHES & OLESCH 1986, ZILBERFARB & NATHAN 1986). Contact rocks developed between younger granite and older ultrabasic rock can be considered as a thermal-metasomatic hornfels-type formation, whereas contact rocks between older granite (or granite-type) and younger ultrabasic rock are classic

examples of metasomatosis products. Hydrothermal alteration, brittle tectonic episodes, and weathering often obscured primary contact rock textures and compositions. In that case, the sequences and assemblages of layer silicates can be used as a tool for deciphering a succession of geological events. Layer silicates capable of gradual changes in the interlayer are suitable material for reconstruction of the transformation sequences (NAGASAWA & *al.* 1974, NOACK & COLIN 1986, PROUST & *al.* 1986, BEAUFORT 1987, DE KIMPE & *al.* 1987, BUURMAN & *al.* 1988, SHAU & *al.* 1990, DRITS & KOSSOVSKAYA 1990, BETTISON-VARGA & *al.* 1991, SCHIFFMANN & FRIDLEIFSSON 1991, INOUE & UTADA 1991, ROBINSON & *al.* 1993).

GEOLOGIC SETTING

The Jordanów-Gogołów serpentinite massif is considered to be a lower part of the Ślęża Paleozoic ophiolitic sequence (MAJEROWICZ 1979, NARĘBSKI & *al.* 1982, NARĘBSKI & MAJEROWICZ 1985), dated either as *c.* 350 Ma (PIN & *al.* 1988), or as *c.* 420 Ma (OLIVER & *al.* 1993).

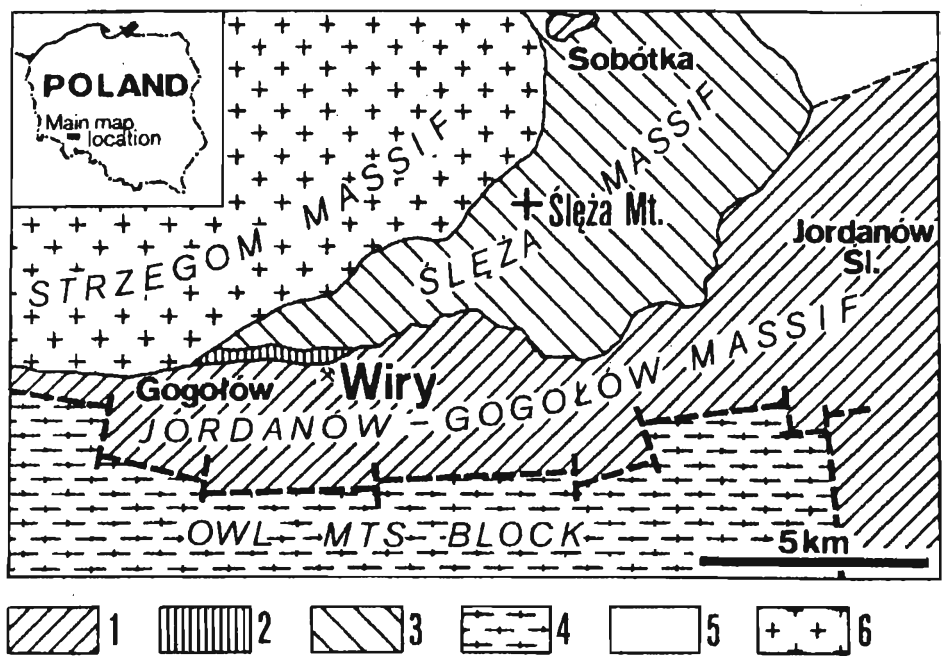

Fig. 1. Geologic sketch-map of the western and central parts of the Jordanów-Gogołów serpentinite massif (*after* MAJEROWICZ 1981; *modified*) in Lower Silesia, Poland

1-3 – OPHIOLITIC SEQUENCE: 1 – mantle tectonites – peridotites, often highly serpentinized, 2 – ultramafic peridotitic cumulates, 3 – gabbros and amphibolites (mafic cumulates, sheeted dykes, and their metamorphic equivalents)
4 – Gneisses of the Owl Mts block, 5 – siliceous slates and phyllites, 6 – Variscan Strzegom granitoid

The Strzegom granitoids represent granodiorites in its central and western parts and granites (including more alkaline, leucocratic, and two-mica varieties) in the eastern part of the massif. Moreover, regular vein aplites are commonly associated with pegmatites. Aplogranites, rocks intermediate between granites and aplites, but rarer than the latter, also occur within the Strzegom granites (PENDIAS & WALENCZAK 1956, KURAL & MORAWSKI 1968).

Several occurences of blastocataclastic or blastomylonitic K-rich leucocratic rocks (locally labelled by a German name *Weißstein*) were found within the Jordanów-Gogołów serpentinites (TEISSEYRE & *al.* 1957, DUBIŃSKA & SZAFRANEK 1990).

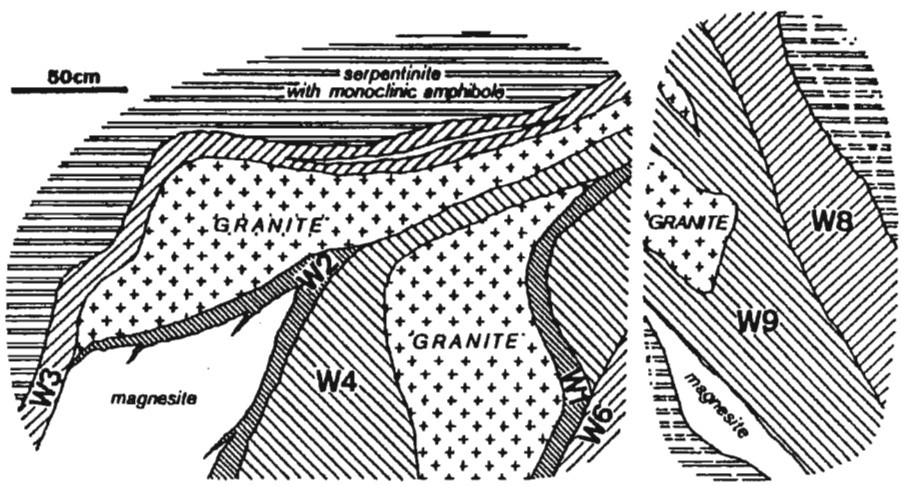

Fig. 2. Selected pegmatite/serpentinite contacts at the mine of Wiry

Samples *W1-W4*, *W6*, and *W7* comprise vermiculite ± interstratified mica/vermiculite ± mica (as major phases), and represent products of the trioctahedral mica alteration; sample *W9* contains chlorite and their transformation products (*after* JELITTO & *al.* 1991)

Serpentinites from western part of the Jordanów-Gogołów massif were locally injected with leucocratic veins exposed in the Wiry mine (GAJEWSKI 1970). The veins are surrounded by mica-chlorite-talc zones, usually highly altered (HARAŃCZYK & WALA 1970; HARAŃCZYK & PROCHAZKA 1974; KOSZELA 1984; JELITTO & *al.* 1991, 1993; SACHANBIŃSKI 1993; JANECZEK & SACHANBIŃSKI 1995).

The age of the magnesite deposit, although apparently younger than that of the granite, is not known accurately (GAJEWSKI 1970). Slip surfaces suggest magnesite formation before the youngest (Alpine?) brittle tectonics episode. Magnesite from Wiry was precipitated from solutions of meteoric origin containing biogenic carbon (JĘDRYSEK & HALAS 1990). Details on geology of the region are given by GAJEWSKI (1970), MAJEROWICZ (1972, 1981), MAJEROWICZ & PIN (1994), and NARĘBSKI (1994).

Peridotite, highly serpentinized and intergrown by magnesite, is the essential country rock in the Wiry area. Serpentinites, unless highly intergrown by a fine-grained carbonate and monoclinic colorless amphibole, display pseudomorphic textures (Pl. 1. Fig. 2). Contacts between leucocratic bodies and ultrabasic rocks are characterized by their diversity and the apparently chaotic distribution of mineral assemblages (Text-fig. 2). Intense brittle tectonics sometimes resulted in splitting contact zones and leucocratic bodies, which are hidden at present (Text-fig. 3). Shear zones in serpentinite commonly contain talc and/or clinochlore, often obliterated by silica-group minerals (opal, chalcedony with its variety chrysoprase, and quartz; *see* Pl. 4, Fig. 3).

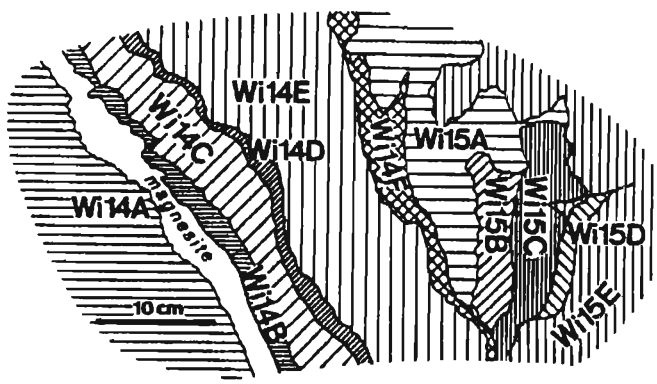

Fig. 3. Schist zone probably resulted from detachment of contact schists from granite-type rock and their tectonic disruption; *Wi14A—Wi15E* are sample numbers

After examination of twelve contact zones, the following main groups of rocks were distinguished.

(*i*) Serpentinites usually overgrown by tremolite and dissected by a network of magnesite (± dolomite ± calcite) veinlets;

(*ii*) Pegmatoid (albitite) veins often dismembered by tectonic event(s) into separate blocks;

(*iii*) Rocks rich in layer silicates (vermiculite, chlorites, interstratified mica/vermiculite, trioctahedral micas *etc*, serpentines exclusively), usually containing an admixture of a monoclinic amphibole, apatite, magnetite and hematite as well as rare titanite and ilmenite;

(*iv*) Veins of massive magnesite partly dismembered into blocks;

(*v*) Shearing zones cutting the serpentinite and comprising talc ± chlorite ± monoclinic amphibole;

(*vi*) A network of veins, veinlets and patches of sepiolite, smectite, and silica minerals.

SAMPLES

The samples, collected at the Wiry underground mine and numbering ninety, represent exocontact assemblages from the leucocratic rock/serpentinite (serpentinized peridotite) boundary. Granites, different vein rocks and pegmatites from the Strzegom massif, serpentinites and *Weißsteine* of the Jordanów-Gogołów massif were used as a background sample set in this study.

Hand specimens of the contact rocks are soft, friable and commonly fine-grained; samples usually contain an admixture of flakes up to 2 mm in diameter; in naked eye the flakes are frequently inhomogeneous, brownish, greenish, and grayish. However, well pronounced schistosity, inherited from the parent rock, is still easily distinguishable. The fragments rich in amphiboles are harder, rough, and whitish in color. Leucocratic rocks are highly tectonized with schist fragments filling the fissures. Pockets of apatite prisms up to 1 cm in diameter, and magnesite spots and veinlets are often found.

METHODS

Minerals were identified using a combination of the X-ray diffraction patterns and microprobe determinations. All parts of the macroscopically inhomogeneous samples were checked separately. The serpentines were identified using the WICKS' & O'HANLEY's (1988) optical criteria for distinguishing the serpentine textures formed after olivine and pyroxene, as well as routine *XRD* powder method.

SEM observations were made with a *Jeol-JSM-840A* electron microscope equipped with an energy-dispersive X-ray detector allowing qualitative chemical analysis. Fresh samples as well as specimens after ultrasonic treatment were used in this study.

XRD identification of layer silicates was performed on oriented specimens using *DRON-1* and *DRON-2A* diffractometers and CoKa radiation. Grain fractions from < 2 μm to coarse flakes were examined. Samples were saturated with Na^+-ions, heated, and treated with liquid ethylene glycol. Oriented preparations were heated on a homemade thermal stage and their X-ray tracings were recorded at temperatures of 75, 150 and 250°C. The tracings were collected using the *DRONEK* program (MUSIAŁ 1992).

Deconvolution of the overlapped diffraction bands was performed assuming Gaussian peak profiles. MÉRING's (1949) diagrams modified by DRITS & SAKHAROW (1976) were used to a preliminary estimation of component types and concentrations in the structures, and REYNOLDS' (1985) *NEWMOD 2* program was used to simulate diffractograms. Calculated patterns of raw and ethylene glycol-treated samples display good conformity with experimental tracings and are similar to the published data (*e.g.* NISHIYAMA & *al.* 1979; REYNOLDS 1980, 1988; ROBINSON & *al.* 1993; BEAUFORT & MEUNIER 1994). The authors calculated about 170 patterns, including the simulations of tracings corresponding to contracted interstratified minerals.

Microprobe determinations were performed using a *JEOL* electron microprobe, 15 KeV, 35 nA, *ZAF* correction procedure, synthetic silicate as well as natural mineral standards. Some samples were analyzed by means of an *ARL* electron microbrobe, 15 KeV, 15 nA, beam spot 2-6 μm. Specimens for microprobe were prepared as polished sections of bulk rocks or coarse grained phyllosilicate flakes (free of fine-grained material), and amphibole prisms mounted in epoxy.

Bulk rock chemical analyses of thirteen samples were performed for major, minor and trace elements by *ICP/MS* and *INAA* methods; Nb was determined by *XRF*.

Fluid inclusions were studied in double-polished 0.05-0.3 mm thick sections for recognition of the fluid inclusions in minerals. Homogenization temperature (*Th*) measurements were made with use of either a heating/freezing microscope stage in air/nitrogen medium or a silicon-oil-immersion heating stage, that could operate up to 290°C with immersion objectives to 100x, as described by KARWOWSKI & *al.* (1979). The accuracy of the *Th* measurements was ±1°C for temperatures up to 200°C and ±1.5°C for temperatures 200-400°C, when the gas-medium stage was used. Immersion heating stage yielded results of the accuracy ±1.5°C (to 150°C) or ±2°C (150-290°C). Freezing runs to obtain freezing (*Tfrz*) and eutectic (*Te*) temperatures of inclusions, were made with accuracy ±0.1°C for temperatures +10 to −22°C and ±0.3°C at lower temperatures. Both stages were calibrated for melting points of a number of pro analysi grade chemical compounds. More than 40% of the investigated inclusions were opened in a *Chaixmeca* microscope crushing stage.

RESULTS AND DISCUSSION

TEXTURES AND CHEMICAL COMPOSITION OF MINERALS

The pegmatoids from Wiry usually consist of major chess-board plagioclase close in composition to albite (Table 1) and minor apatite. Fragments of tectonically included mica (micaceous mineral) and/or chlorite schists are commonly found (Pl. 1, Fig. 1).

Set of schists rich in layer silicates (vermiculite, chlorites, interstratified mica/vermiculite, trioctahedral micas, *etc*, exlusively of serpentines, Pl. 3, Fig. 1 *and* Tables 2-3) developed at the expense of pseudomorphic and bastite-containing serpentinites. The latter have been evidenced by small grains of magnetite arranged parallel to the former (100) partings of pyroxene, perfectly preserving ghosts of the pyroxene exsolution lamellae (Pl. 2, Fig. 1).

Compositions of phlogopite, interstratified mica/vermiculite and vermiculite from schists vary mainly in potassium and magnesium contents, whereas K/Fe^{3+} (total) ratios do not vary both in regional and in single sample scale (Text-figs 4-5).

Formation of the contact zones was concomitant to tectonic episodes; thus any regular sequence of mica-chlorite-talc zones is absent at the Wiry mine. As a result, the tectonized chlorite schist could be displaced to mica zone and intergrown by younger mica flakes (at present often their transformation product), that originated due to an increase of the mica zone thickness (Pl. 3, Fig. 2). Similar process seemed to produce inhomogeneous large flakes composed of chlorite surrounded by epitaxial vermiculite-like mineral (without transitional stages, *see* Text-fig. 6), and sealed with fine-grained matrix of vermiculite-like mineral (Text-fig. 7 *and* Pl. 6, Figs 1-3).

Schists, composed of layer silicates, comprise diversified amount of a monoclinic amphibole (Text-fig. 8), which seems to be younger than chlorite, talc, and mica (Pl. 2, Fig. 2). Almost monomineral amphibole schists were also

Table 1
Representative analyses of feldspars and amphiboles from the studied area

Sample	Feldspars		Amphiboles		
	Wi4A	Wi4A	Wi15E	Wi14E	Wi41
SiO_2	67.70	65.42	0.00	45.45	42.84
TiO_2	-	-	0.08	0.27	0.70
Al_2O_3	19.01	21.50	0.19	10.20	14.53
Cr_2O_3	-	-	-	-	0.13
FeO	0.02	0.12	1.29	8.39	9.61
MnO	-	-	0.08	0.27	0.09
NiO	-	-	0.12	0.01	-
MgO	0.01	-	24.82	17.20	14.74
CaO	1.71	2.67	13.16	12.55	12.09
BaO	0.12	-	n.d.	n.d.	n.d.
K_2O	0.84	0.14	-	0.60	0.48
Na_2O	10.14	10.03	0.04	1.75	2.59
total	99.55	99.88	98.53	96.69	97.80
	on the basis of 8 oxygens		*on the basis of 23 oxygens*		
Si	2.99	2.88	7.93	6.63	6.22
Ti			0.01	0.03	0.08
Al	0.99	1.12	0.03	1.75	2.49
Cr					0.01
Fe^{2+}tot.			0.15	1.02	1.17
Mn			0.01	0.03	0.01
Ni			0.01		
Mg			5.00	3.74	3.19
Ca	0.08	0.13	1.90	1.96	1.88
K	0.05	0.01	-	0.11	0.09
Na	0.87	0.86	0.01	0.49	0.73

n.d. - not determined

Table 2
Representative analyses of layer silicates (I) from the studied area

Sample	Chlorites		Serpentine
	Wi12A	Wi35	Wi12A
SiO_2	29.83	28.72	43.97
TiO_2	-	-	-
Al_2O_3	21.52	21.10	0.05
Cr_2O_3	-	0.01	-
FeO	6.39	9.66	0.69
MnO	0.02	0.41	-
NiO	0.10	-	0.07
MgO	30.45	25.62	41.00
CaO	-	0.05	0.05
K_2O	0.03	0.05	0.04
Na_2O	-	0.03	-
total	88.34	85.65	85.87
	on the basis of 14 oxygens		
Si	2.81	2.84	4.11
Al^{IV}	1.19	1.16	
Al^{VI}	1.20	1.31	
Fe^{2+}tot.	0.50	0.80	0.05
Mn		0.03	
Ni	0.01		
Mg	4.28	3.78	5.71
tot. oct.cat.	5.99	5.92	5.76

found. The amphibole composition ranges from tremolite to pargasite (Table 1). Tremolites from Wiry show well-constrained chemical compositions, which occupy separate fields (Text-figs 9-10). In other amphiboles, both Al- and Ti-concentrations increase, and Mg/(Mg+Fe) ratio decreases with increasing (K+Na)-content (Text-fig. 10). Both groups of amphiboles can be found in one sample. The occurrence of Na- and K-bearing amphiboles at Wiry is related to the contact zones; tremolite is a common admixture both in the contact schist and in serpentinites (P. BYLINA, *personal communication* 1994), in the latter suggesting the tectonic displacement of serpentinite fragments into metasomatic contact zone.

Veinlets, pockets, and coatings consisting of small rhombohedral crystals of magnesite (Pl. 5, Fig. 2) were ubiquitous; veins of almond- and cone-shaped

Table 3
Representative analyses of layer silicates (II) from the studied area

	Mica	Hydrobiotite	Vermiculites		
Sample	Wi4A	Wi37	Wi14D	Wi34	Wi35
SiO_2	38.64	37.45	35.08	40.33	37.97
TiO_2	0.11	-	0.63	0.03	tr
Al_2O_3	17.58	13.64	12.72	10.94	14.35
Cr_2O_3	-	-	0.05	-	-
FeO	9.93	6.42	6.40	4.28	7.58
MnO	0.54	0.19	0.07	0.09	0.14
NiO	-	-		0.22	0.04
MgO	17.39	22.55	22.68	23.97	23.45
CaO	-	-	0.56	0.07	0.10
K_2O	9.50	4.38	0.12	0.13	0.26
Na_2O	0.58	0.34	0.03	0.27	0.20
total	94.27	85.01	78.34	80.33	84.09
on the basis of 11 oxygens					
Si	2.84	2.91	2.83	3.13	2.85
Ti	0.01		0.04		
Al^{IV}	1.16	1.09	1.17	0.87	1.15
Al^{VI}		0.17	0.04	0.13	0.12
Fe^{3+}tot.			0.43	0.28	0.47
Fe^{2+}tot.	0.61	0.42			
Mn	0.03	0.01			
Ni				0.01	
Mg	1.90	2.62	2.72	2.77	2.62
Ca			0.05		
K	0.89	0.43	0.01	0.01	0.03
Na	0.08	0.05		0.04	0.02
tot. oct.cat.	2.91	3.22	3.24	3.19	3.24

tr - traces

calcite (Pl. 4, Fig. 1 *and* Pl. 5, Fig. 3), and dolomite-magnesite intergrowths (Pl. 5, Fig. 4) were also present in the studied samples. Accessory native gold occurs in carbonate-rich fragments of schists, which are a listwaenite-type rock (Text-fig. 11).

Some samples consist of large flakes almost completely covered by spongy coatings (Pl. 4, Fig. 2) being composed of smectite (JELITTO & *al.* 1993) which forms intergrowth with magnesite (Pl. 5, Fig. 1). The carbonates seem to be formed after the large flakes formation.

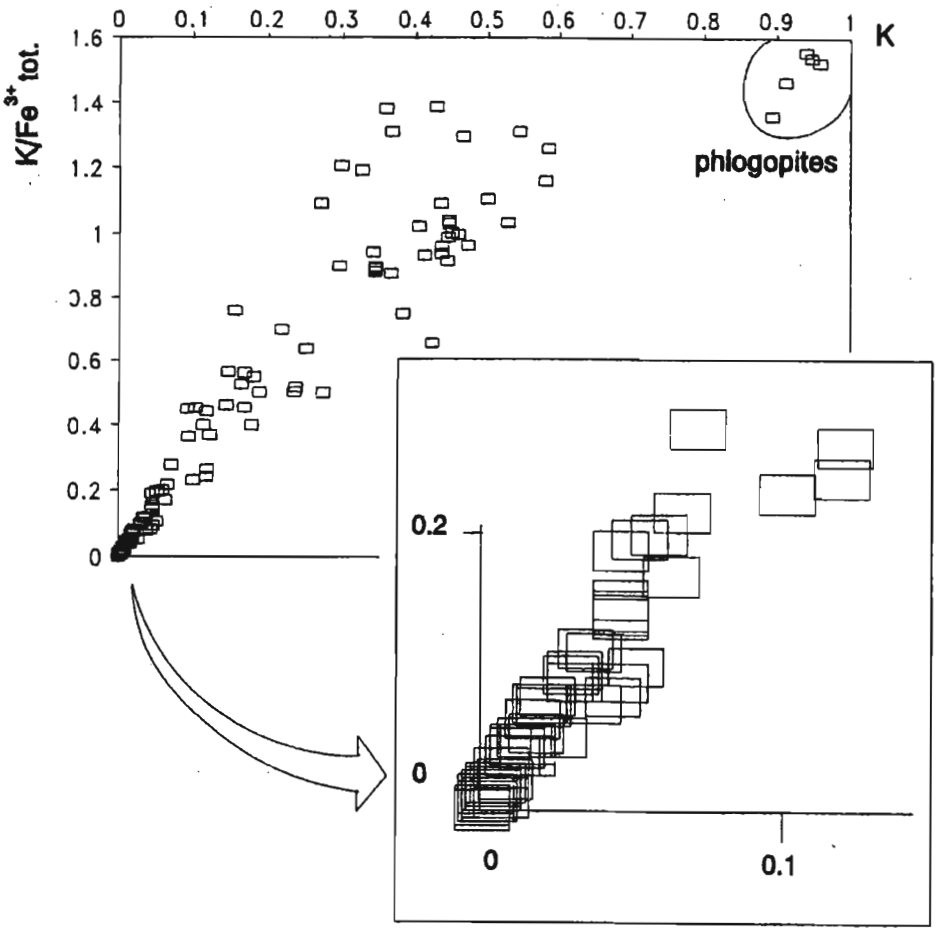

Fig. 4. Plots of K content *versus* $K/Fe^{3+}tot.$ ratio in coarse flakes of layer silicates (micas, vermiculites, chlorites, various interstratified minerals, and their intergrowths) from the contact schist from Wiry

The microprobe analyses were calculated assuming constant tetrahedral composition $[Si_3Al]$ *pfu*; arrow points the enlarged lower left fragment of the upper plot

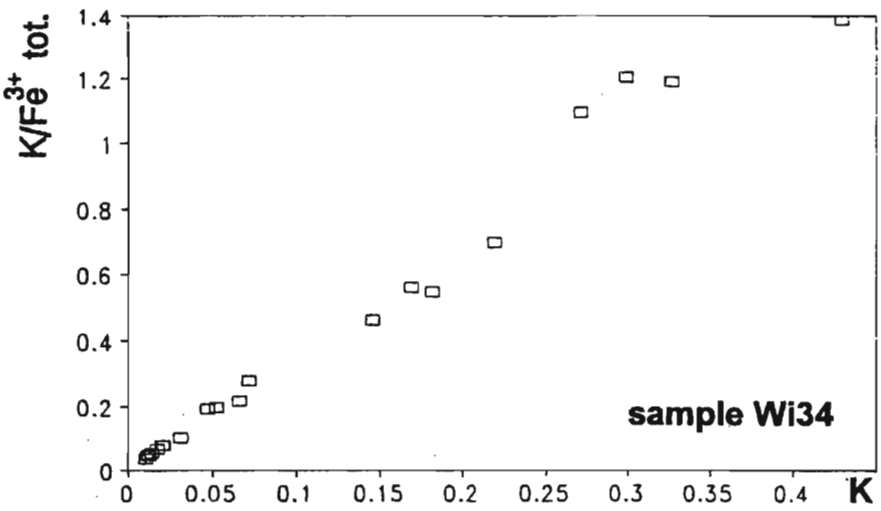

Fig. 5. Plot of K content *versus* K/Fe^{3+} tot. ratio in coarse flakes of layer silicates (a vermiculite-like mineral is the major phase, *see* Text-fig. 14 for details); sample *Wi34*

The microprobe analyses were calculated assuming constant tetrahedral composition [Si_3Al] *pfu*

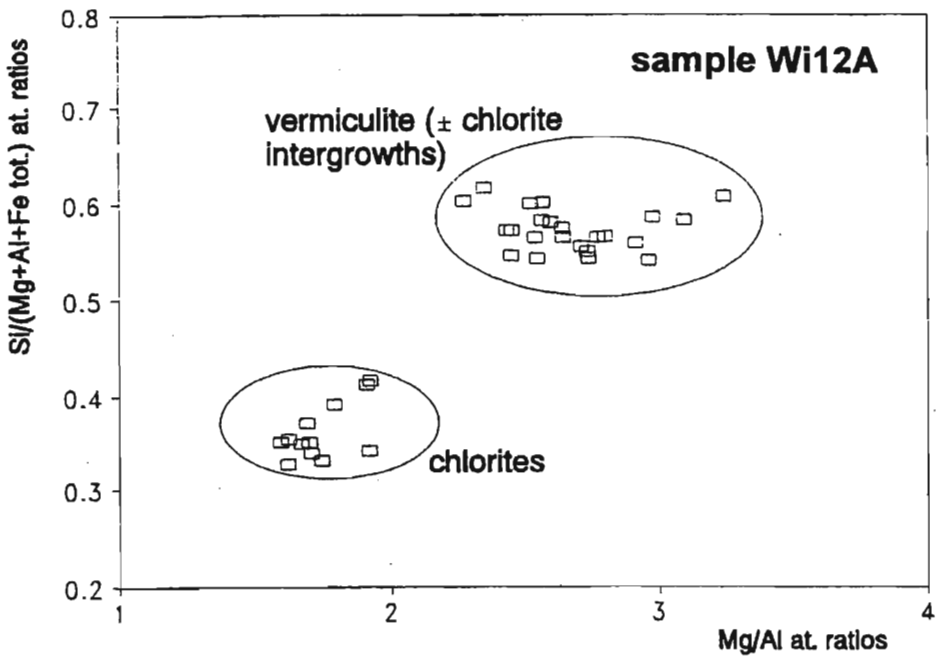

Fig. 6. Plot of Mg/Al ratio *versus* Si/(Mg+Al+Fe tot.) in inhomogeneous flakes (*cf.* Text-fig. 7 *and* Pl. 6, Figs 1-3); sample *Wi12A*

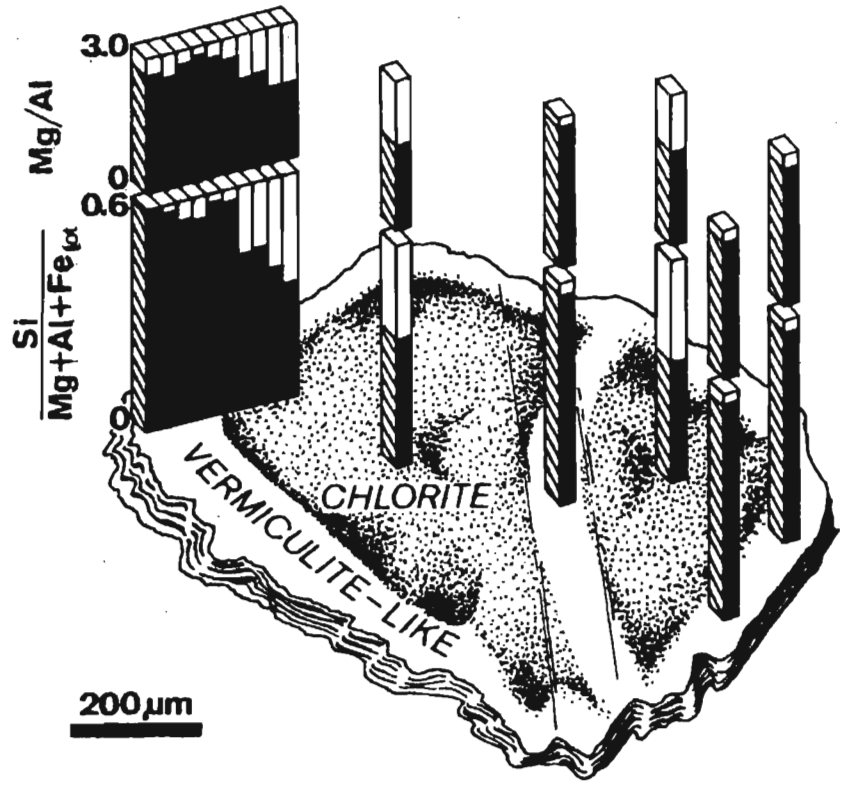

Fig. 7. Inhomogeneous flake with discontinuous variations of Mg/Al and Si/(Mg+Al+Fe tot.) ratios (*cf.* Pl. 6, Fig. 1)

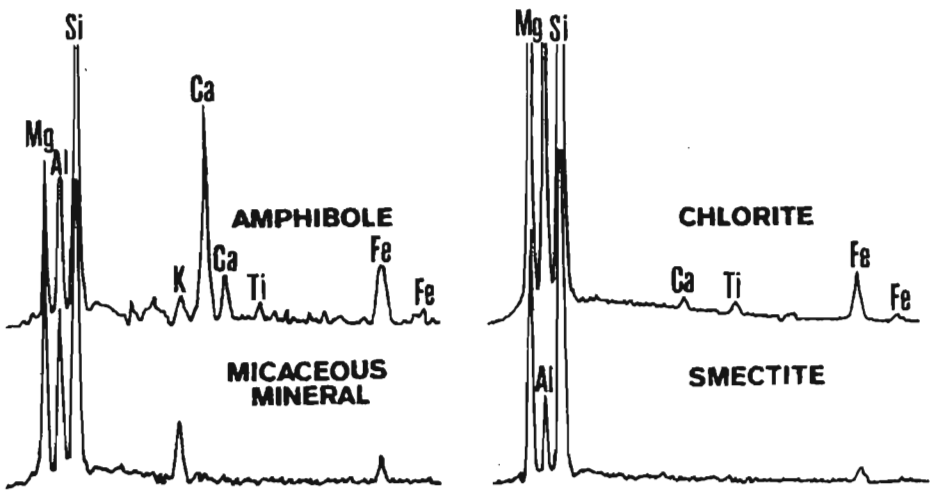

Fig. 8. Energy-dispersive X-ray spectra of major minerals from the contact zones at Wiry

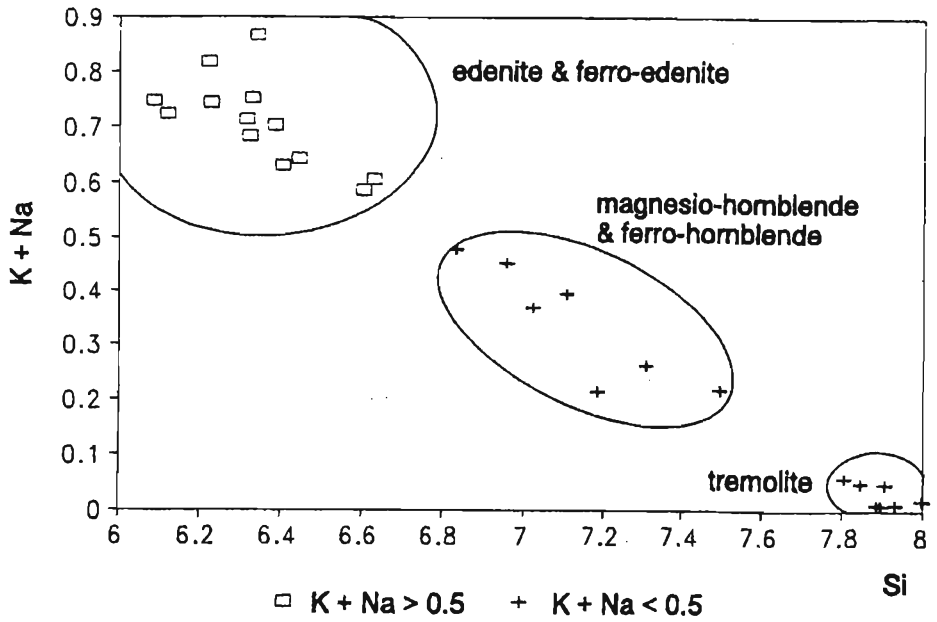

Fig. 9. Chemical compositions of monoclinic amphiboles from the contact schist from Wiry
Microprobe analyses were calculated on the basis of 23 oxygens

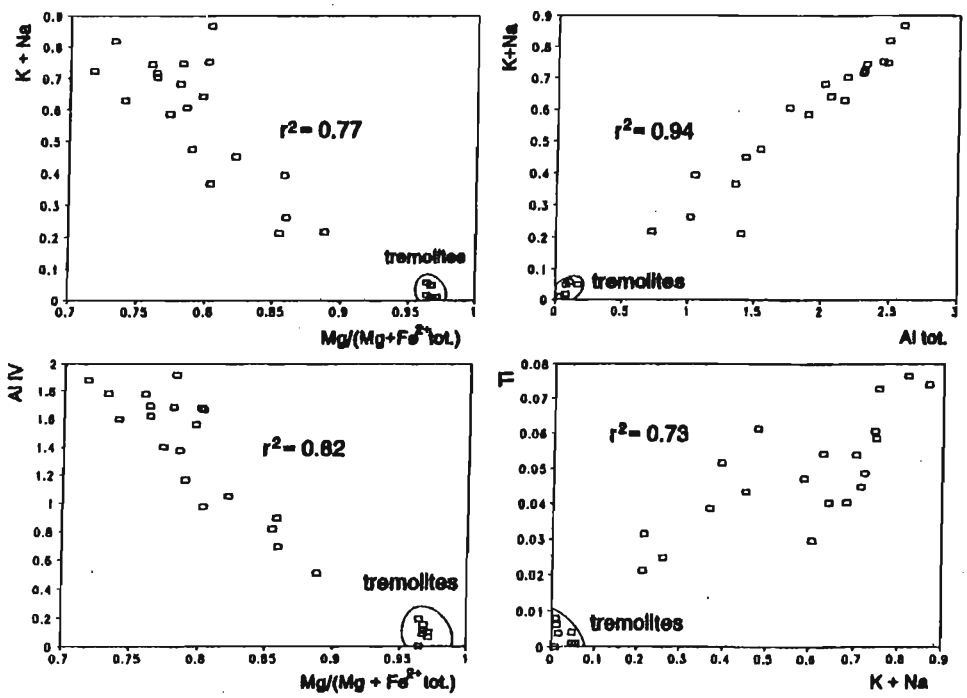

Fig. 10. Ranges of chemical compositions of amphiboles from the contact schist from Wiry
Microprobe analyses calculated on the basis of 23 oxygens; *r* denotes linear correlation coefficient, tremolite compositions not included

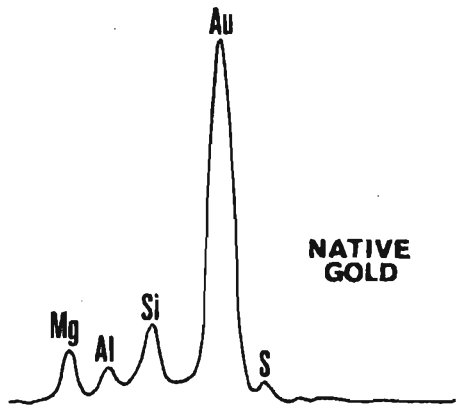

Fig. 11

Energy-dispresive X-ray spectrum of an accessory native gold inclusion in vermiculite-like flake (minor Mg, Si and Al contamination); sample *Wi33*

The schistosity and tectonically deformed of flakes persisted formation of magnesite and alternation of layer silicates (Pl. 4, Fig. 1).

ROCK COMPOSITION

The bulk rock composition of pegmatoid from Wiry (Table 4) differs from Strzegom granites and *Weißstein* from Tąpadła (Jordanów-Gogołów serpentinite massif) in relatively high Na_2O and Al_2O_3, *versus* low K_2O and SiO_2 concentrations. Trace elements compositions in the pegmatoid contrast with those of the reference granites, *e.g.* Rb-, Cs-, Ba-, Y-, and REE-contents are relatively low, whereas Sr- and Be-concentrations are high (Table 5). It is thought that Rb, Cs, and Ba could migrate with K from the pegmatite during formation of the contact zones, while Sr and Be contents seem to reflect primary concentrations of these elements in the pegmatite. This composition suggests the pegmatoid origin related to desilification and potassium depletion, thus a probable hybridal origin.

Chemical compostion of serpentinite from Wiry (Table 4) is typical of other serpentinites of the Jordanów-Gogołów serpentinite massif (Niśkiewicz 1970). Talc and chlorite schists from shearing zones also represent similar bulk rock chemical compositions (Tables 4-5).

Major and trace element contents in the contact zone schists were distinctly influenced both by the parent serpentinite composition (relatively

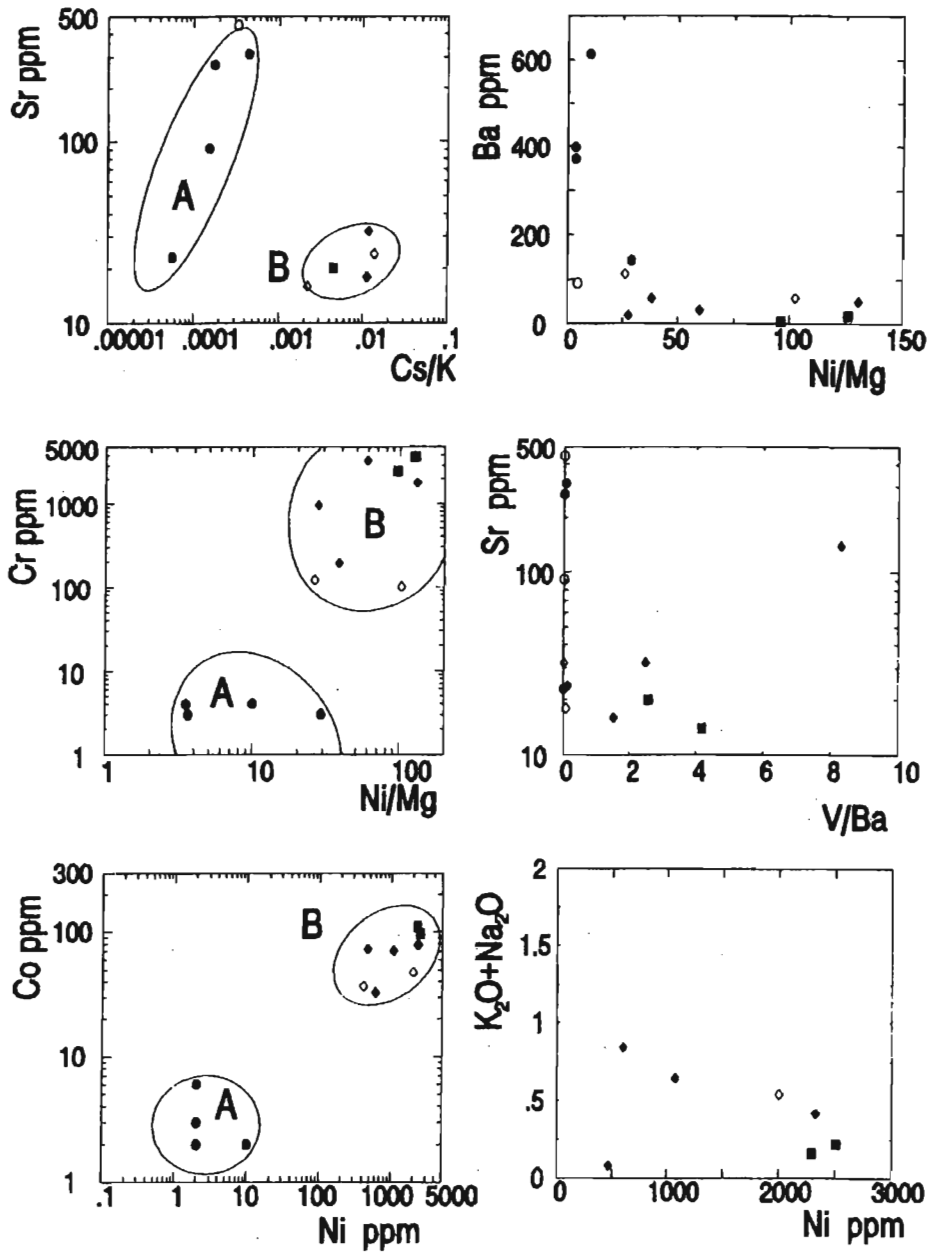

Fig. 12. Bulk chemical composition of the selected rocks from the Wiry mine and adjacent areas

A — Leucocratic rocks, B — serpentinites and rocks formed due to their alteration; **circle** — albite rock from Wiry, **solid circle** — granites from the Strzegom massif and *Weißstein* form Tąpadła, **solid square** — serpentinites from the western part of the Jordanów-Gogołów massif, **diamond** — contact schists, **solid diamond** — talc and chlorite schists

Table 4
Bulk rock analyses (major elements) from the studied area

Sample	Serpentinites		Talc schist	Chlorite schists	
	Wi26s	Go1	Wi26t	Wi30	W8*
SiO_2	41.77	41.10	49.78	29.44	28.30
TiO_2	0.01	<0.01	0.04	0.08	0.30
Cr_2O_3	0.56	0.36	0.01	0.50	0.26
Al_2O_3	2.12	0.86	1.14	16.82	17.78
Fe_2O_3tot.	8.76	7.35	1.60	7.60	8.72
MnO	0.07	0.12	0.02	0.08	0.16
NiO	0.32	0.29	0.25	0.14	0.30
MgO	33.08	39.50	32.36	29.76	29.56
CaO	0.61	0.75	0.28	0.16	0.16
Na_2O	0.14	0.09	0.50	0.58	0.36
K_2O	0.08	0.07	0.04	0.06	0.06
P_2O_5	<0.01	<0.01	0.12	0.10	0.12
ignition loss	13.21	8.88	11.96	13.96	12.62
total	100.75	99.36	98.10	99.26	99.90

* - altered rocks
Ch7 - granite from Chwałków (the eastern part of the Strzegom-Sobótka granitoid massif); Ch7E - hornblende- and biotite-rich xenolith from granite Ch7; Go1 - highly serpentinized peridotite from Gogołów (the western part of the Jordanow-Gogołów serpentinite massif); St5 - granodiorite from Strzegom (the western part of the Strzegom-Sobótka granite massif)

Contact schists			Granites and related rocks				
Wi27*	Wi34*	Wi37*	Wi4Ag	Ta1	St5	Ch7	Ch7E
28.42	36.58	34.88	64.88	77.14	73.02	73.04	68.35
2.89	0.02	0.04	<0.01	0.06	0.26	0.25	0.54
0.14	0.03	0.02	tr.	tr.	tr.	tr.	tr.
13.13	10.62	11.60	19.86	12.47	12.42	14.46	15.55
11.89	4.56	5.24	1.02	0.29	2.44	1.74	3.61
0.15	0.12	0.14	<0.01	<0.01	0.05	0.04	0.10
0.06	0.08	0.05	tr.	tr.	tr.	tr.	tr.
27.96	25.84	25.86	0.70	0.57	0.94	0.33	0.91
1.15	0.52	1.06	0.98	0.20	1.51	1.56	2.36
0.08	0.34	0.44	9.84	4.80	3.29	4.13	4.88
<0.01	0.50	2.14	0.55	3.87	3.99	3.64	1.30
0.89	0.40	0.72	0.13	0.04	0.12	0.05	0.16
12.16	19.18	16.65	0.69	<0.01	1.09	0.51	1.06
98.92	98.73	98.84	98.46	99.45	99.14	99.75	98.84

Ta1 - *Weißstein* from Tąpadła (mylonite recrystallized to a granophyre-like texture); Wi4A - plagioclase (An 4-23) rock with tectonically included apatite and phlogopite assemblage; W8, Wi27, Wi34, Wi37 - vermiculite±chlorite±interstratified mica/vermiculite±mica interstratified chlorite/vermiculite (smectite) contact schists

Table 5
Minor elements in bulk rock samples from the studied area

	Serpentinites		Talc schist	Chlorite schists	
Sample	Wi26s	Go1	Wi26t	Wi30	W8*
Rb	<10	<10	<10	<10	7.6
Cs	3	<0.5	3.9	<0.5	1.1
Cu	7	3	2	2	3
Ag	0.4	0.6	<0.4	<0.4	<0.4
Au	8	5	<5	<5	<5
Be	<2	<2	<2	<2	<2
Sr	20	14	20	32	16
Ba	19	5	58	32	50
Zn	46	38	16	59	98
Th	<0.5	<0.5	<0.5	<0.5	11
U	1.4	<0.5	3.5	<0.5	1.5
Sc	14	8.1	0.7	30	23
Y	<1	<1	12	20	32
La	0.3	<0.2	0.3	0.3	7.6
Ce	<3	<3	<3	<3	18
Nd	<5	<5	<5	<5	7
Sm	<0.1	<0.1	<0.1	<0.1	1.2
Eu	<0.1	<0.1	<0.1	<0.1	<0.8
Tb	<0.5	<0.5	<0.5	<0.5	<0.5
Yb	<0.1	<0.1	<0.1	<0.1	0.6
Lu	<0.05	<0.05	<0.05	<0.05	0.08
Pb	<5	<5	<5	<5	<5
Zr	37	31	38	34	270
Hf	<0.5	<0.5	<0.5	<0.5	2.2
As	21	13	10	<2	3
Sb	<0.2	0.7	0.3	0.9	0.3
Bi	6	<5	<5	<5	<5
V	49	21	2	80	76
Nb	<2	<2	<2	2	12
Ta	<1	<1	<1	<1	2
Cr	3800	2500	100	3400	1800
Co	96	110	48	71	79
Ni	2513	2287	2000	1073	2326

Se <3 ppm, Br <1 ppm, Cd <0.5 ppm, Hg <1 ppm, Se <3 ppm, Mo <5 ppm, W <3 ppm

Contact schists			Granites and related rocks				
Wi27*	Wi34*	Wi37*	Wi4Ag	Ta1	St5	Ch7	Ch7E
<10	133	546	<10	97	168	121	78
3.9	57	200	<2	1.8	5.1	5.3	4.8
31	37	2	2	5	2	2	2
0.6	<0.4	<0.4	0.6	<0.4	<0.4	<0.4	<0.4
<5	<5	<5	<5	10	<5	<5	<5
<2	4	3	114	2	2	2	3
139	24	18	447	23	91	271	312
20	58	112	92	142	371	614	398
87	130	181	9	2	46	25	59
9.6	1.5	1.0	0.7	7.6	13	12	6.6
<0.5	1.4	1.3	<0.5	1.4	7.0	3.8	8.4
29	4.5	4.5	0.2	2.6	5.0	4.2	7.9
6	26	28	<1	23	24	4	15
101	<0.2	0.3	<0.2	7.9	33.8	22.9	23.5
194	<3	<3	<3	17	65	42	44
91	<5	<5	<5	6	24	16	18
11	<0.1	0.1	<0.1	2.5	5.1	3.8	4.6
1.5	<0.1	<0.1	<0.1	<0.1	0.9	0.6	0.8
<0.5	<0.5	<0.5	<0.5	1.0	<0.5	<0.5	0.9
0.9	<0.5	<0.5	0.6	1.6	2.0	1.5	2.6
0.17	<0.05	<0.05	<0.05	0.25	0.27	0.24	0.31
8	<5	<5	6	39	17	14	<5
400	51	132	36	45	205	125	190
7.3	3.9	2.5	1.5	1.4	5.2	3.0	4.7
2	<2	<2	<2	<2	<2	<2	<2
0.3	1.1	3.7	<0.2	<0.2	0.2	<0.2	0.5
<5	<5	<5	<5	<5	<5	<5	<5
166	9	11	2	2	10	11	27
129	56	76	2	8	22	16	28
6	75	76	2	2	2	<1	2
960	190	120	<2	3	4	4	3
73	33	37	<1	2	3	2	6
466	598	408	2	10	2	2	2

high concentrations of Cr, Ni, and Co), and by elements released from pegmatite, mainly K, Rb, Cs, Ba (*see* Tables 4-5 *and* Text-fig. 12). Moreover, contact schists are enriched in P, Nb and Ta, what can be considered as a common result of the granite-derived fluids activity (*cf.* FERSMAN 1953). Neither fresh nor altered rocks from contact zones yielded any accumulation of Ni, nor any increase of Ni/Mg ratio (Text-fig. 12). At Wiry, the diversified concentrations of V and Mn are not well constrained, although *e.g.* MARSHALL & MANCINI (1994) found a significant depletion of vanadium in analogous zones at Vammala (Finland).

X-RAY CHARACTERISTICS OF PHYLLOSILICATES

The following layer silicates were recognized at Wiry: mica, smectite, vermiculite, chlorite, talc, serpentinite, interstratified mica/vermiculite, chlorite/smectite, three component interstratified mica/vermiculite/chlorite, and chlorite/swelling chlorite/smectite (JELITTO & *al.* 1993).

Some samples rich in vermiculite (plus minor mica) contained quasi-regulary interstratified mica/vermiculite, recognized on the basis of almost rational series of 001 reflections in the natural sample: 24.5, 12.63, 8.2, 4.88,

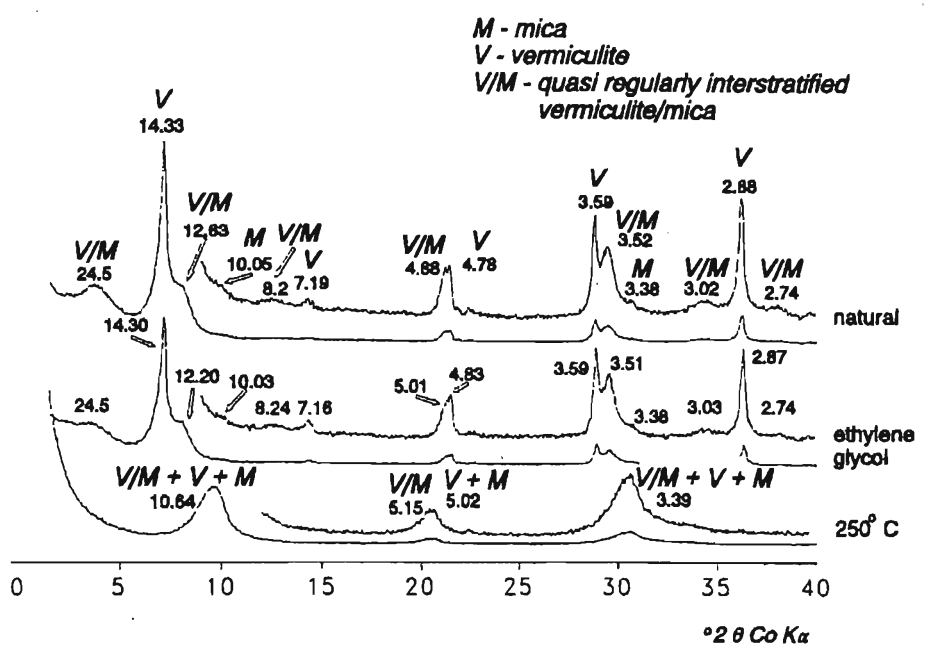

Fig. 13. X-ray tracings of coarse-grained flakes from sample *Wi37*

Oriented aggregates; *d*-values were determined by deconvolution of the experimental patterns; some of the peaks are hidden (overlapped by high intensity and/or large peaks); satisfactory deconvolution of large maximum 10.64Å was not possible

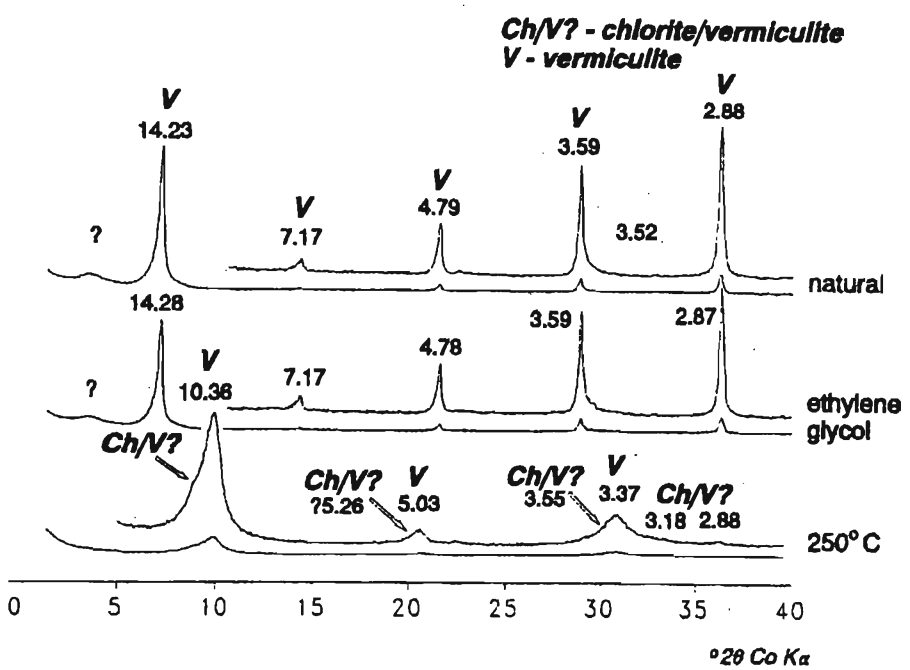

Fig. 14. X-ray tracings of coarse-grained flakes from sample *Wi34*

Oriented aggregates; *d*-values were determined by deconvolution of the experimental patterns; some of the peaks are hidden (overlapped by high intensity and /or large peaks); satisfactory deconvolution of large maximum 10.36Å was not possible

3.52, 3.02, 2.7 Å, with coefficient of variability $cv = 1.37$ (Text-fig. 13), where *cv* was calculated according to BAILEY (1982). The expansion of mixed-layer mineral after ethylene glycol treatment (24.5, 12.10, 8.24, 5.01, 3.51, 3.03, 2.74 Å, $cv = 1.05$; *see* Text-fig. 13) at first glance suggests high layer charge of vermiculite layers in the mixed-layer mineral (DE LA CALLE & SUQUET 1988). After heating of the sample at 250°C (using heating stage), the incompletely contracted 10.64 Å structure was produced (Text-fig. 13). The X-ray patterns were recorded after four hours of pre-heating and without cooling the specimen, thus spontaneous rehydration of the vermiculite and vermiculite layer in the interstratified phase should not have to occur (WADA & *al.* 1990). Hence, this result should be interpreted as an admixture (*c.* 15%) of non-contracting (chlorite?, intergrade chlorite-vermiculite?) layers in the interstratification, thus the mineral probably represents a three-component interstratified structure composed of mica(50%)/vermiculite(35%)/chlorite(15%) layers. Similar, three-component (mica/vermiculite/chlorite; 60%, 15%, and 25%, respectively) mixed layer mineral from Wiry was recently described by JELITTO & *al.* (1993). Nevertheless, an incomplete dehydration of both vermiculite and vermiculite layers in the interstratified phase cannot be excluded (COLLINS & *al.* 1992).

According to the routine *XRD* determinations, high-charge (expanding up to *c.* 14.3 Å after ethylene glycol treatment) vermiculite seems to be the most frequent mineral in coarse-grained flakes of the studied samples (Text-fig. 14). However, after heating its collapsation was not complete (to *c.* 10.4 Å) and an admixture of irregularly mixed-layer chlorite/vermiculite (hidden in both natural and glycolated samples due to overlappings of the basal reflections) was also recognized. An admixture of K-bearing flakes (mica and/or interstratified mica/vermiculite; *see* Text-fig. 5) was not found during the X-ray study. The partial contraction of vermiculite-like mineral is ambiguous. Either its contraction could result from admixture od chloride layers in the vermiculite-like phase, or it reflects partial dehydration of vermiculite; the first interpretation is more convincing.

The fine-grained fraction contains less vermiculite and more mixed-layer chlorite/vermiculite and chlorite than coarse flakes (Text-fig. 15). This vermiculite contracts after heating to 10.03 Å, but its swelling to 14.75 Å after glycol saturation suggests a high-charge vermiculite/low charge vermiculite (smectite?) interstratification.

Chlorite-to-vermiculite layers ratios in the interstratified chlorite/vermiculite was determined by comparing experimental and computed X-ray

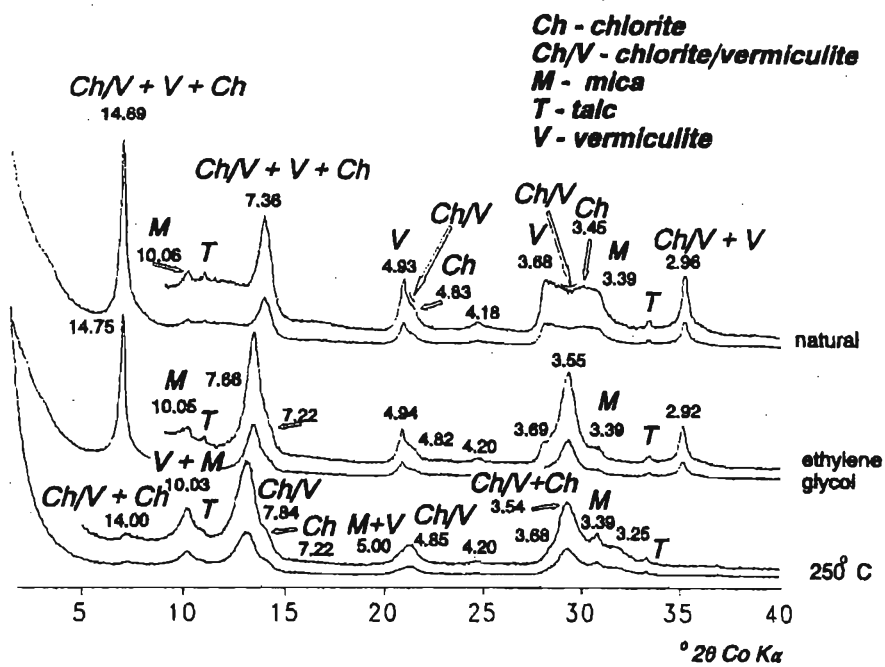

Fig. 15. X-ray tracings of fine-grained fraction (<2 mm) from sample *Wi34*

Oriented aggregates; *d*-values were determined by deconvolution of the experimental patterns; some of the peaks are hidden (overlapped by high intensity and/or large peaks)

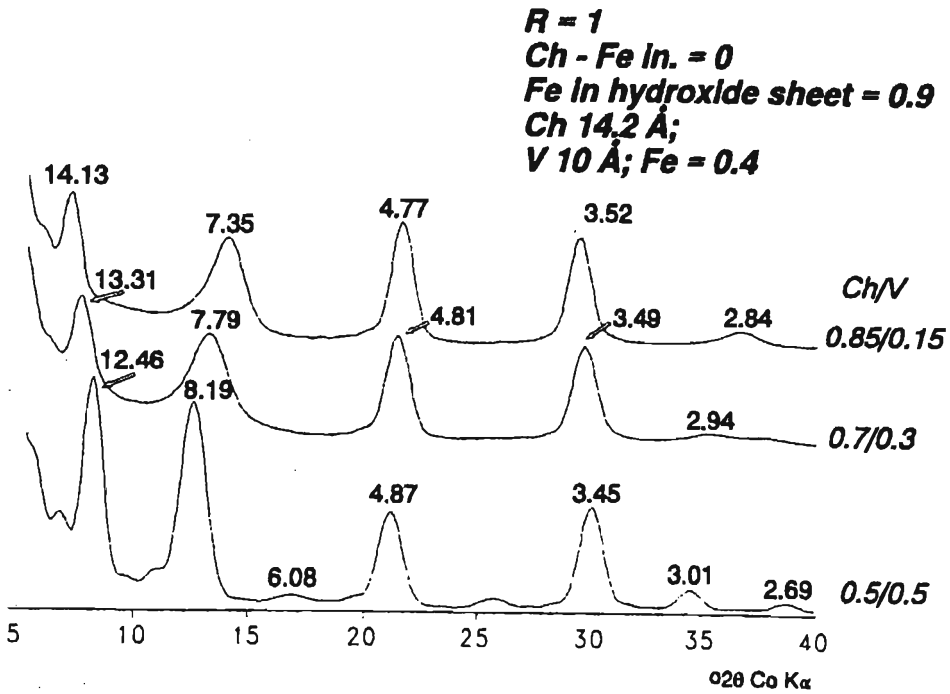

Fig. 16. The *NEWMOD*-calculated *XRD* patterns for a contracted interstratified chlorite/vermiculite; the tracings show positions of diffraction maxima as related to chlorite/vermiculite ratios

Ch — Chlorite with inhomogeneous iron distribution (in — octahedral sheet of talc-like layer, Fe=0), V — vermiculite with iron content 0.4 *pfu* calculated on the basis of $[O_{10}(OH)_2]$, Ch/V — chlorite/vermiculite ratio in the interstratified mineral; R — *Reichweite*

patterns, and assuming the microprobe-determined vermiculite and chlorite compositions as representative ones. The best conformity of reflection positions was obtained for $R = 1$ (*R* — *Reichweite*, the most distant layer, in an interstratified sequence, that affects the probability of occurrence of the final layer; *see* REYNOLDS 1980) and chlorite-to-vermiculite ratio equal 0.7/0.3 (Text-fig. 16). The relative intensities of the experimental and calculated peaks of heated samples disagree so significantly that an asymmetric distribution of iron between the talc-like layers and brucite-like inner sheet of chlorite is considered (Text-fig. 17). The fitting of the calculated and experimental tracings still was not satisfactory; a better approximation was achieved for a high Fe content in the chlorite layers in the interstratified mineral, higher than the Fe content in the regular chlorite from Wiry (Text-fig. 18). The relative intensity of the *c.* 4.8 Å reflection at experimental tracing is still lower than at the calculated one.

Another variety of interstratified chlorite/vermiculite was detected in the fine-grained fractions of the studied samples (Text-fig. 19). The mineral can be tentatively identified as interstratified chlorite(85%)/vermiculite(15%). Regard-

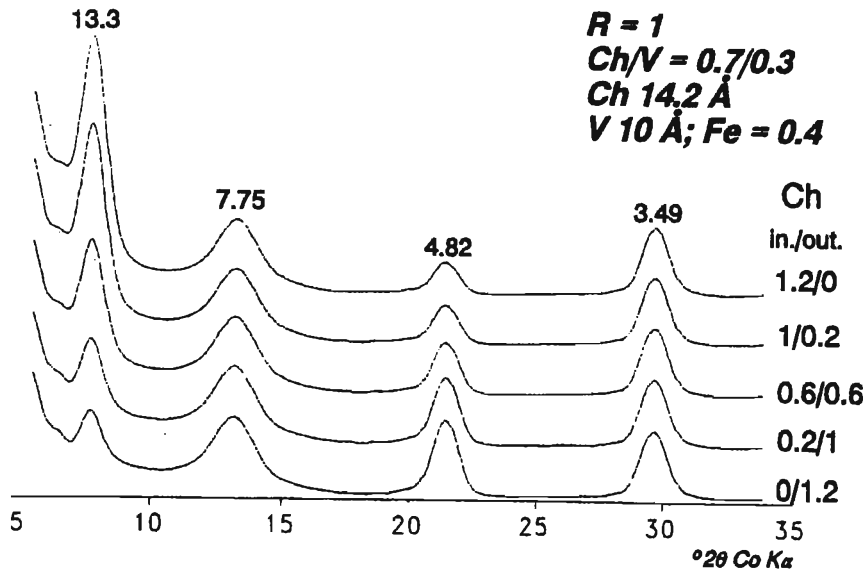

Fig. 17. The *NEWMOD*-calculated *XRD* patterns for a contracted interstratified chlorite/vermiculite; the tracings show intensities of basal diffraction maxima as related to iron distribution between octahedral sheets of a talc-like layer (*in.*) and a brucite-like sheet (*out.*) in chlorite layers; for other abbreviations *see* Text-fig. 16

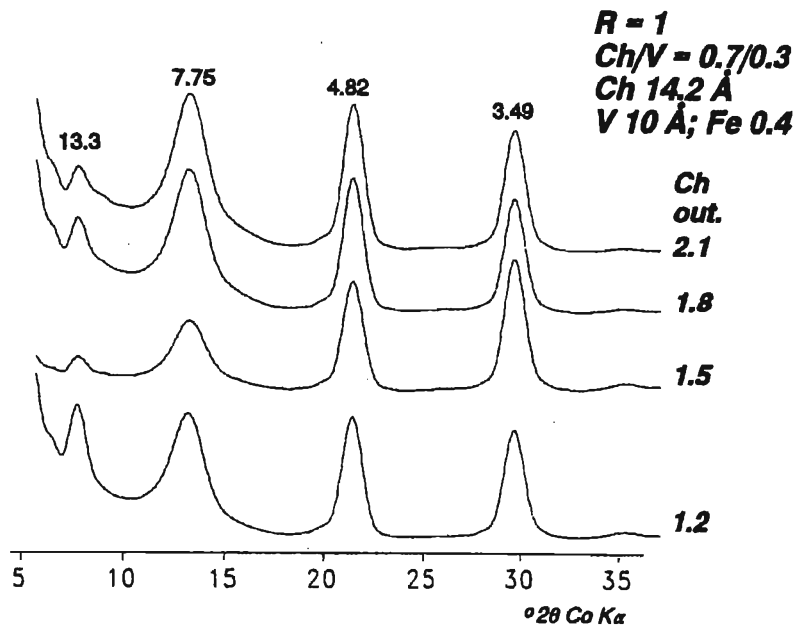

Fig. 18. The *NEWMOD*-calculated *XRD* patterns for a contracted interstratified chlorite/vermiculite with asymmetric iron distribution in chlorite layers; the tracings show intensities of basal diffraction maxima as related to iron content in a brucite-like sheet in chlorite layers; for abbreviations *see* Text-figs 16 *and* 17

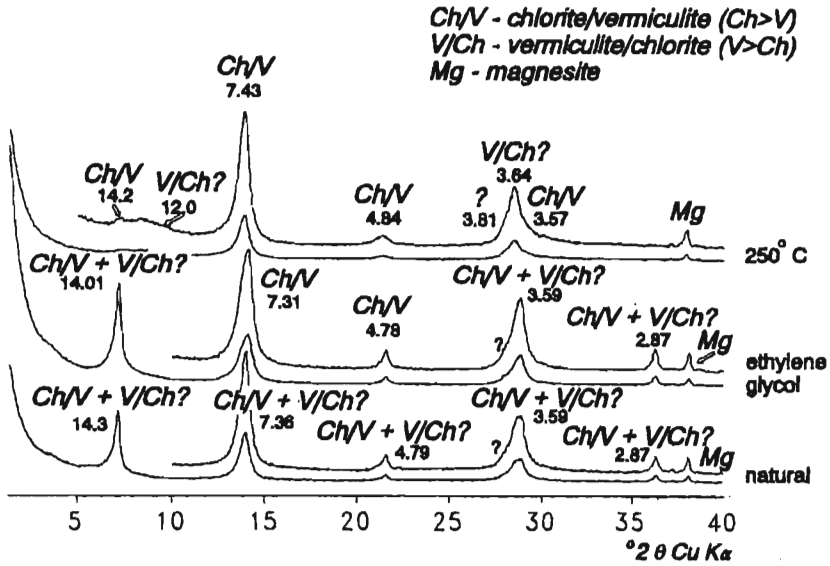

Fig. 19. The X-ray tracings of fine-grained fraction (<2 mm) from sample *Wil4D*

Oriented aggregates; *d*-values were determined by deconvolution of the experimental patterns; some of the peaks are hidden (overlapped by high intensity and/or large peaks)

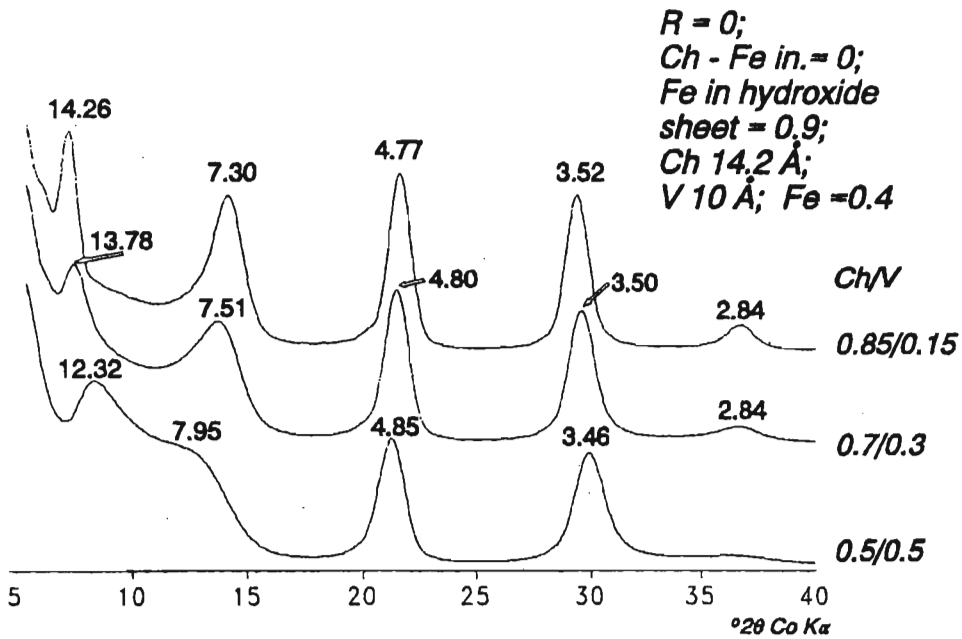

Fig. 20. The *NEWMOD*-calculated *XRD* patterns for a contracted interstratified chlorite/vermiculite with asymmetric iron distribution in chlorite layers; the tracings show positions of diffraction maxima as related to the chlorite/vermiculite ratios; for abbreviations *see* Text-figs 16 *and* 17

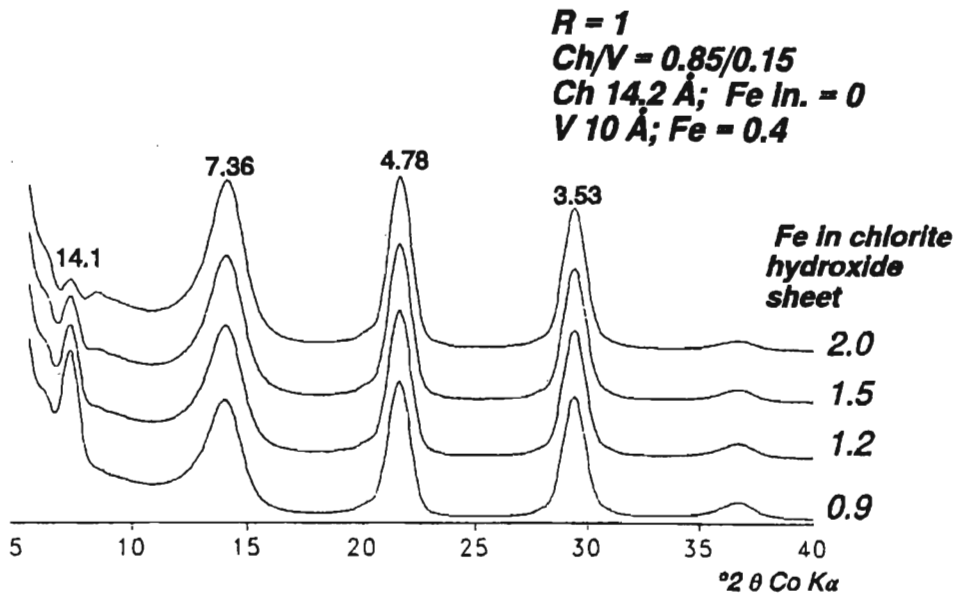

Fig. 21. The *NEWMOD*-calculated *XRD* patterns for a contracted interstratified chlorite/vermiculite with asymmetric iron distribution in chlorite layers; the tracings show intensities of basal diffraction maxima as related to iron content in a brucite-like sheet in chlorite layers; for abbreviations *see* Text-figs 16 *and* 17

less the used value of *R* (0 or 1), the calculated X-ray patterns were almost identical (Text-figs 16 *and* 20). If the above chlorite-to-vermicuite ratio in the interstratified mineral is accepted, a merely satisfactory conformity of experimental and calculated X-ray peak intensities (the 14 Å reflection intensity lowering) can be achieved supposing the high iron content and its extremely asymmetric distribution, *i.e.* the total Fe location in the brucite-like sheet (Text-fig. 21). However, the calculated relative intensities of the *c.* 4.8 Å reflections are still too high.

Coarse-grained flakes from the studied samples (vermiculite, interstratified vermiculite/mica, chlorite, mica) are trioctahedral and their 060 reflections range 1.541-1.544 Å.

JELITTO & *al.* (1993) identified the followig polytypes by means of oblique texture method (WIEWIÓRA & WEISS 1985, WEISS & WIEWIÓRA 1986): (*i*) mica-*1M* (*3T*), (*ii*) vermiculite-*Ia*, and (*iii*) chlorite and some "intergradient" chlorite/vermiculite-*IIb* (*after* BAILEY 1984). Potassium saturation of the vermiculites and interstratified minerals containing mica layers produced phlogopite-like structure *1M* (Text-fig. 22).

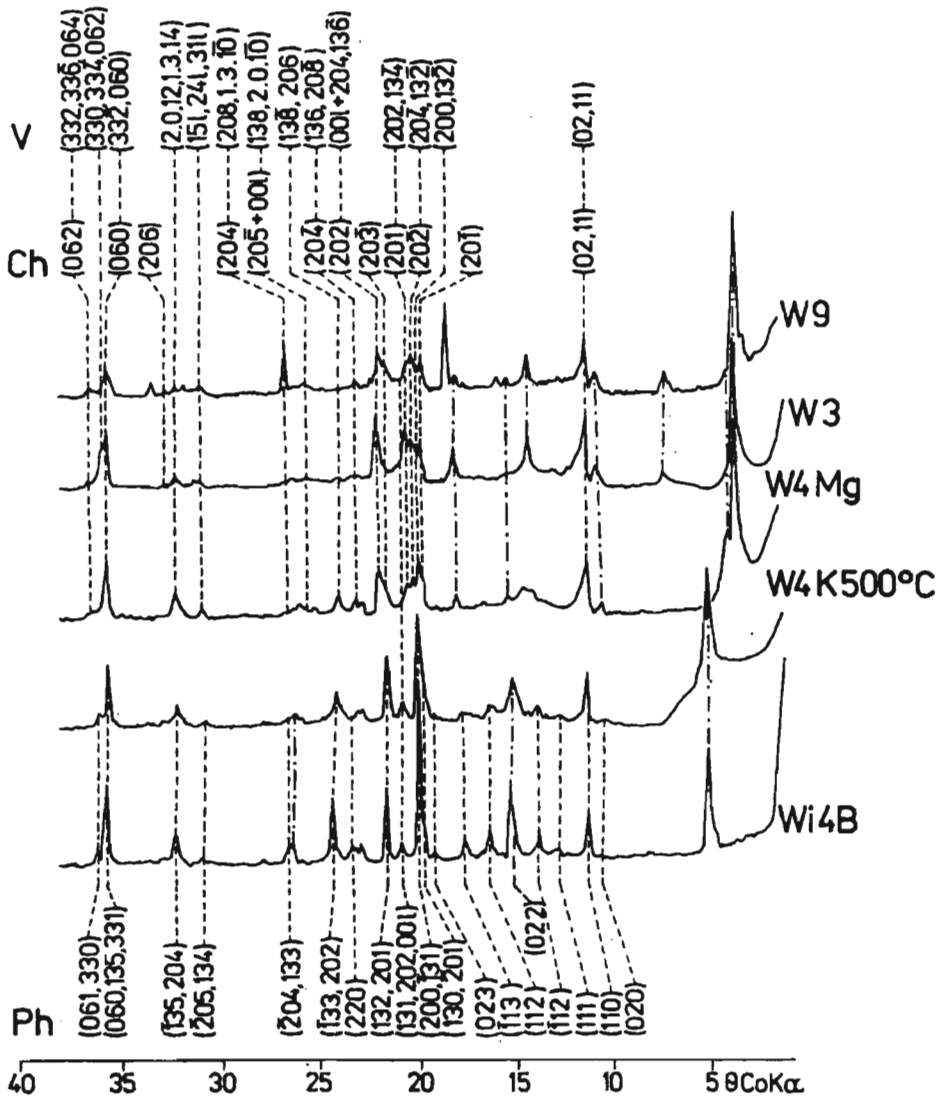

Fig. 22. The *XRD* transmission patterns of the selected samples at $n=90°$

V – Vermiculite-*Ia* ($2M_B$-*VII-meso*), **Ph** – phlogopite-like structure *1M* (*3T*) [$1M_A$-*I* ($3T_A$-*IV*)] produced after heating of the K^+-saturated sample *W4 K500°C* or natural phlogopite from Wiry (*Wi4B*), **Ch** – chlorite-*IIb* (subfamily *C*); indices and polytype notation after Bailey (1984), in parantheses polytype notation according to Wiewióra & Weiss (1985), and Weiss & Wiewióra (1986); unlabelled maxima represent (001) reflections, *after* Jelitto & *al.* (1993)

FLUID INCLUSIONS

Fluid inclusions were studied in three groups of minerals from the contact rocks: amphiboles, apatite, and carbonates. All inclusions were very small, usually less than 10 μm in length; only few inclusions achieved 20 μm when tubular or acicular in habit (Text-fig. 23). Inclusions occurred rarely, especially those in size suitable for microscope observations and heating/freezing runs. Frequent cracking and leaking during temperature increase or decrease further diminished the amount of inclusions that yielded valuable data. Inclusions in sixteen samples from the Wiry mine were the source of 120 *Th* and/or *Tfrz* measurements.

Homogenization temperatures of primary inclusions in amphiboles fall in two distinct groups: 303-276°C (14 measurements) and 255-229°C (18 measurements). These inclusions were found mainly in greenish hornblende-type amphibole; three inclusions that occured in tremolite homogenized in the high-temperature ranges. Inclusions in apatite homogenized at temperatures 260-242°C (14 measurements), similar to the low-temperature range of the inclusions in amphibole. Dolomite and calcite bear inclusions of *Th* 197-162°C (25 measurements); calcite grains contained also primary inclusions that homogenized at 109-42°C (35 measurements) and one-phase low-temperature inclusions. All the inclusions, except for the last ones, were two-phase and homogenized in liquid phase. Inclusions in magnesite were not found.

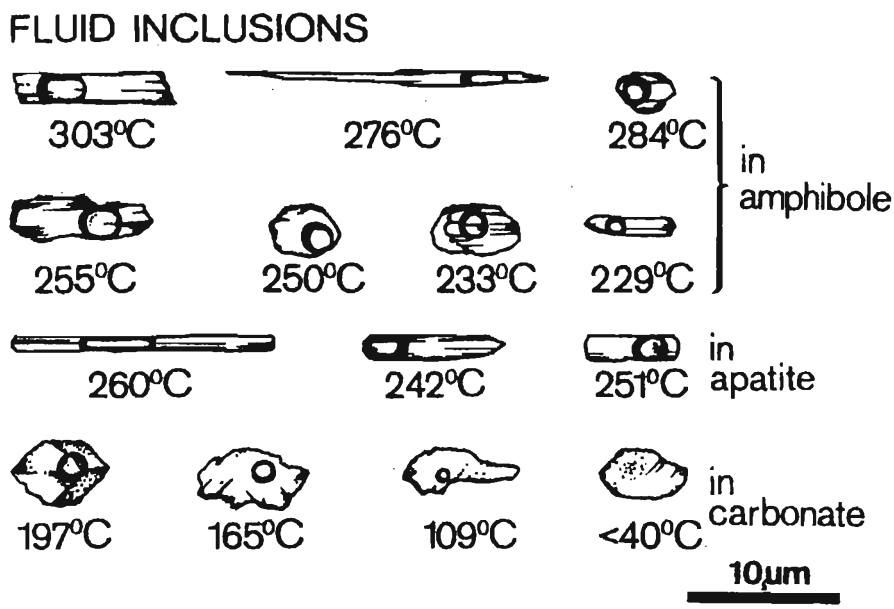

Fig. 23. Fluid inclusions hosted by minerals of the contact assemblages at Wiry

Fluid inclusions in the silica group minerals, especially in chrysoprase, found in the specimens collected at Wiry and in the abandoned mine of Szklary at the neighboring ultrabasic massif, yielded two *Th* values of 97 and 114°C, and on the basis of the inclusion-to-bubble volume proportion *Th* for a number of other inclusions were evaluated as ranging from 70 to 120°C (Kozłowski & Sachanbiński 1984).

Freezing runs of fluid inclusions were the source of information on compositions and concentrations of the inclusion fluids (Potter & *al.* 1978, Crawford 1981, Hall & *al.* 1988, Bodnar 1993). Three types of the fluids were found (Text-fig. 24), distinguished on the basis of their eutectic points: $CaCl_2$-NaCl-H_2O (*Te* −52°C), NaCl-H_2O (*Te* −20.8°C) and KCl-NaCl-H_2O solutions (*Te* −22.9°C).

Observations of the inclusion fillings of low salt concentrations at the eutectic temperatures sometimes did not yield unambiguous results, thus certain $CaCl_2$- and especially KCl-bearing solutions might have been considered as pure NaCl-H_2O fluids. Nevertheless, the NaCl-H_2O compositions were also undoubtedly ascertained. Inclusions in amphiboles contained fluids of total salt concentrations 2.7-16.7 wt. %, the NaCl share was from 1.9 to 15.3 wt. %, $CaCl_2$ — up to 4.3 wt. % and KCl up to 3.6 wt. % (72-100, 0-28 and 0-22 wt. % of the total salts, respectively). Inclusions in apatite were filled with $CaCl_2$-NaCl-H_2O fluid of total salt concentrations 13.2-18.0 wt. %, NaCl share 4.6-14.9 wt. % and $CaCl_2$ — 2.4-9.9 wt. % (35-83 wt. % NaCl in total salts, *i.e.* sometimes $CaCl_2$ was the prevailing salt component). High-temperature

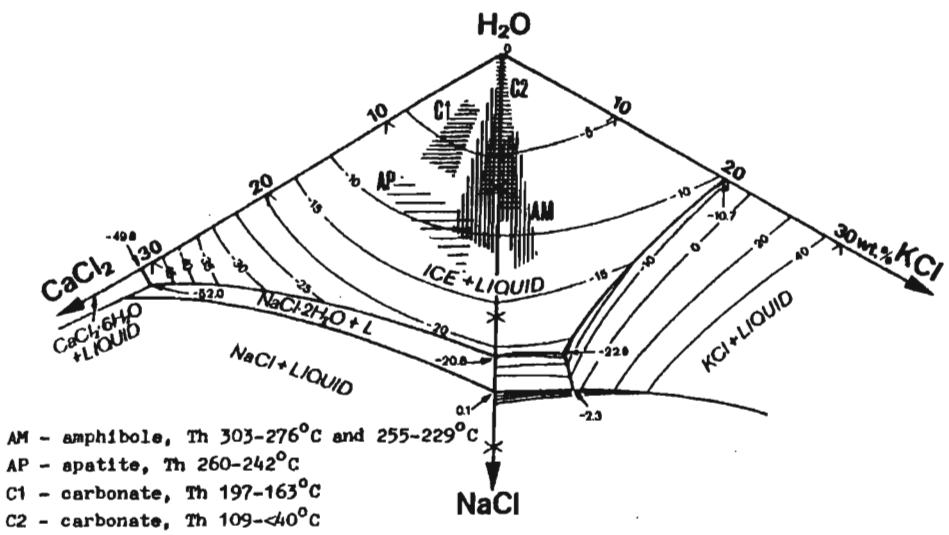

Fig. 24. Compositions of liquid phase of the inclusions in amphibole, apatite, and carbonates

The phase diagrams taken from Crawford (1981); *note*, the two triangular diagrams are separate plots, not two faces of a tetrahedral plot

carbonates: calcite and dolomite, yielded similar fluid data though of lower concentrations: 5.0-11.4 wt. %, total salts dissolved comprised 1.9-7.3 wt. % NaCl and 1.8-7.1 wt. % $CaCl_2$ (38-64 wt. % NaCl in total salts). Inclusions in low-temperature calcite contain essentially NaCl solutions of total salt concentrations from 11.5 to fresh water and with admixtures of $CaCl_2$ up to 1.6 wt. % or KCl up to 1.9 wt. % (up to 15 and 16 wt. % of total salts, respectively).

Carbon dioxide was not observed in the inclusions. Not elucidated sufficiently was also the occurrence of the carbonate and the magnesium ion in

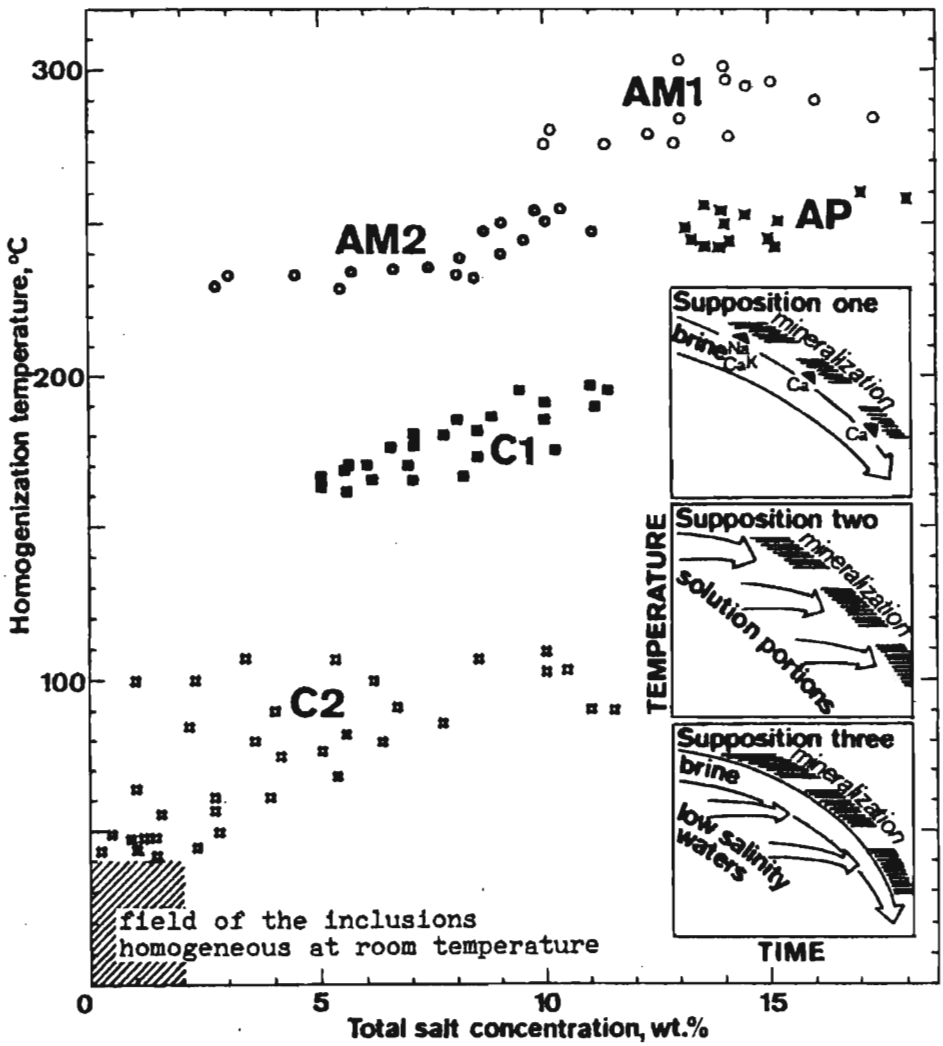

Fig. 25. Salt concentrations in inclusions *versus* homogenization temperatures

Host minerals: *AM1* and *AM2* — amphiboles, *AP* — apatite, *C1* and *C2* — carbonates; the inset diagrams are discussed in the text

the parent solutions. Apparently, carbonate ions were a deficient component of the late stage fluids that formed dolomite, calcite, and magnesite but did not reach a high concentration that could be detected by freezing methods. The aqueous chloride systems with magnesium ions yield no distinctive phenomena on freezing, in the presence of relatively high concentrations of sodium and calcium (*see* the system description *in* CRAWFORD 1981).

Homogenization temperatures of fluid inclusions, when plotted *versus* total salt concentrations, split in separate groups (Text-fig. 25). The high-temperature inclusions in amphiboles (*AM1*) are the group of the highest salinity; the lower-temperature inclusions in amphiboles (*AM2*) bear fluids of distinctly lower salinity. Inclusions in apatite (*AP*) have salinity similar to that of the inclusion group *AM1* but their *Th* are in ranges of the inclusion group *AM2*. Inclusions in high-temperature carbonates (*C1*) are separated with a *Th* gap from the amphibole and apatite data, but their salinity is in the salinity ranges of the *AM2* inclusion group. Low-temperature carbonates contain inclusions (*C2*) of *Th* essentially below 100°C and within the broadest salinity ranges, from the values typical of the *AM2* group to almost fresh water. The gradual and rather irregular salinity decrease concomitant with temperature lowering is a very general feature of the parent fluids evolution.

Three more detailed suppositions concerning the fluid evolution have been made (Text-fig. 25). Supposition one suggests a single inflow of the parent fluid (Ca-Na-K brine) and its continuous evolution that influenced the composition and concentration of the fluid: first, amphibole crystallization used a part of calcium, sodium, and potassium from the fluid, then apatite and carbonates consumed calcium, and micas did potassium. This model does not explain the final dilution of the NaCl-rich solutions.

Supposition two would imply independent inflows of the solution portions that caused any of the three mineralization stages: **a** — amphiboles and apatite, **b** — high temperature carbonates, **c** — low-temperature carbonates. This scheme would require additional evidence that so distinctly separated mineral-forming media once existed and extincted before the medium of the next stage appeared.

Supposition three presents a pattern, where the early brine that possibly caused the crystallization of amphiboles and apatite, next mixed with low-salinity formation and/or connate waters. These waters could bear carbonate ions and the mixing process probably resulted in early carbonate precipitation. Magnesite formation obviously was not related by a direct mode to this mineral-forming sequence, but might have been caused by late activity of connate waters.

CONCLUSIVE REMARKS

PRESSURES AND TEMPERATURES OF MINERAL FORMATION

Fluid inclusions in the studied minerals did not give any basis to the evaluation of pressures during their formation. Thus, the aluminium-in-hornblende geobarometer (HAMMARSTROM & ZEN 1986, HOLLISTER & *al.* 1987, JOHNSON & RUTHERFORD 1989) was applied.The present authors' considerations led to the selection of the JOHNSON'S & RUTHERFORD'S (1989) calibration plot, and the analysis of amphiboles bearing 1.3 to 1.5 atoms of total aluminium per formula unit (*pfu*). Other amphiboles bearing either more or less aluminium *pfu* did not contain fluid inclusions suitable for studies. The pressures, that on the basis of the present studies can be related to the early stage contact metamorphic process at Wiry, range from 2.1 to 2.6 Kbar (*see* the inset in Text-fig. 26).

The *Th* values of fluid inclusions generally are neither the temperatures of the inclusion sealing nor the temperatures of crystallization of the host minerals. The determination of real crystallization temperature requires the pressure-dependent correction to the homogenization temperature (ROEDDER 1984). The corrections were calculated for *Th* values of inclusions in amphiboles on the basis of the physico-chemical properties of the NaCl aqueous solutions of appropriate concentrations (HAAS 1976a,b; POTTER & BROWN 1976). The crystallization temperature ranges determined on the basis of the *AM1* inclusion group and for the pressure of 2.6 Kbar were 650 to 535°C, whereas the *AM2* inclusion group for the pressure of 2.1 Kbar yielded the crystallization

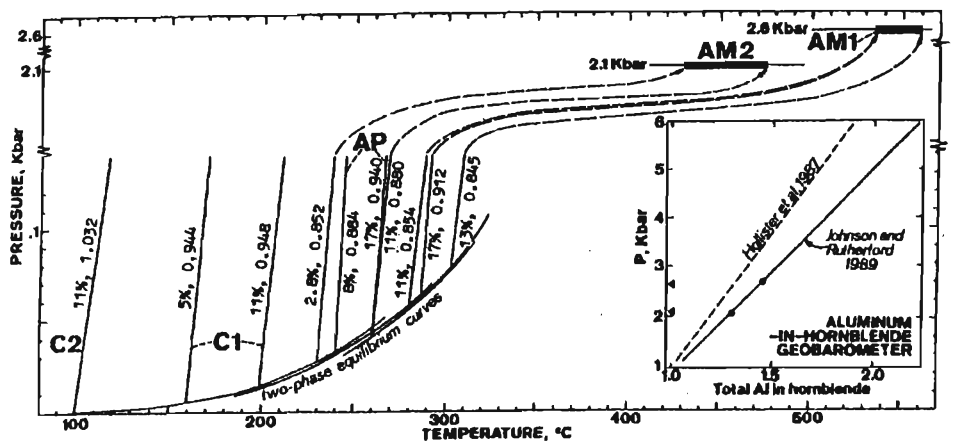

Fig. 26. Isochores of fluid inclusions in amphiboles (*AM1* and *AM2*), apatite (*AP*) and carbonates (*C1* and *C2*), and pressure corrections for *Th* of inclusions in amphiboles, calculated for pressures determined by means of the aluminum-in-hornblende geobarometer (*see* inset)

The physico-chemical properties taken from HAAS (1976a,b), *and* POTTER & BROWN (1977); isochores in g per cm^3

temperatures from 475 to 430°C (Text-fig. 26). The above temperatures concern directly the hornblende amphiboles formed during the contact metamorphism, and probably they can be extended on the apatite crystallization. Carbonates crystallized at lower temperatures (*Th* 197-162°C for *C1*, and ≤109°C for *C2*) and, probably under significantly lower pressures, thus the pressure correction to *Th* also should be low, probably of about few tens centigrades.

SOURCE OF THE HIGH-TEMPERATURE SOLUTIONS

The contact rock assemblage has chemical composition contrasting with that of the parent country rocks, that is the serpentinites. Their formation required an inflow of potassium (hornblende and micas), sodium (hornblende) and calcium (amphiboles, apatite and carbonates). Potassium-bearing solutions are typical of the high temperature post-magmatic fluids that penetrate the crusts of the magmatic granitoid bodies. Subsequently, potassium is replaced

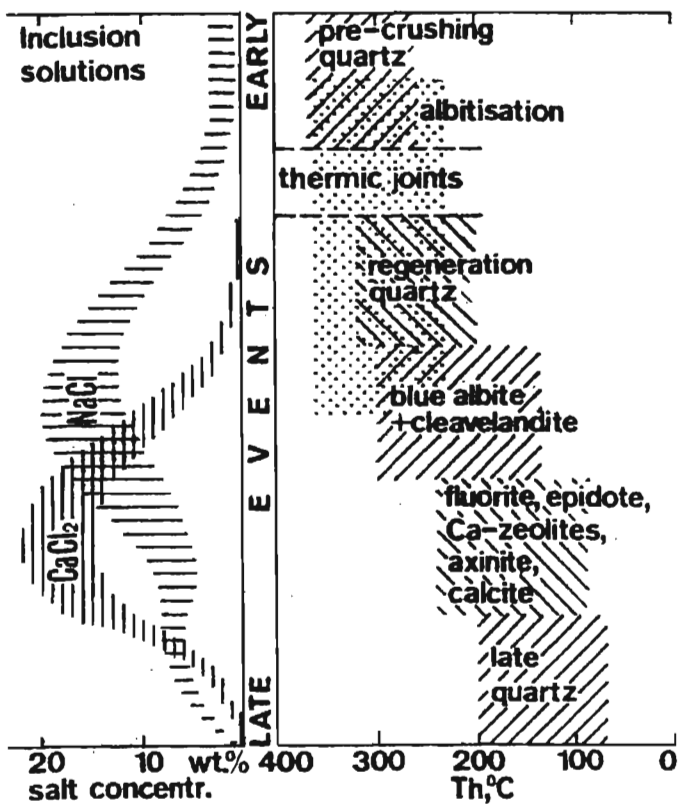

Fig. 27. Evolution of the inclusion solutions in pegmatitic minerals from the Strzegom massif (*from* KOZŁOWSKI 1994)

by sodium in the fluids (*see e.g.* KOZŁOWSKI 1978). Hence, potassium and sodium were probably released from the Wiry pegmatoid veins during their consolidation and hybridization. An increase of calcium concentration fluids seems to be a process analogous to the post-magmatic processes in the Strzegom massif marked by fluid inclusions of *Th* from *c.* 400°C to *c.* 200°C and containing up to 20 wt. % $CaCl_2$ (KOZŁOWSKI 1984, 1994). The studies of fluid inclusions in minerals of the Strzegom pegmatites (Text-fig. 27) revealed that the calcium-rich fluids were frequently replaced by sodium-bearing calcium-poor solutions. A similar sequence was found in the contact assemblages at Wiry. The source of calcium can be found in rock-forming oligoclase in granitoids that at the post-magmatic stage (*Th* 400-300°C) was extensively albitized by sodic fluids (NOWAKOWSKI & KOZŁOWSKI 1984). Thus, it is reasonable to accept the described phenomena as being responsible for the calcium inflow to the exocontact rocks at Wiry.

The hypothesis on the granitoid source of calcium and the granitoid-wallrock interaction scheme presented above has also a consequence that concerns the post-magmatic albitization in the Strzegom granitoid massif. The calcium-bearing fluids migrated from the granitoids toward the exocontact rocks. Thus, the estimated pressures of 2.1-2.6 Kbar should not be higher than the pressure in the granitoid massif during albitization. Hence, these values can be tentatively accepted as an approximate pressure during albitization in the SE part of the Strzegom massif, adjacent to the Jordanów-Gogołów serpentinite massif.

RECONSTRUCTION OF THE CONTACT ZONES

Structures of the contact zones are usually studied taking into account a distance from the leucocratic rock. Undoubtedly, such approach is viable for tectonically undisturbed rocks. If the tectonic distortion was ignored, different mineral assemblages could be improperly explained, *e.g.* as products of local equilibrium variations. On the basis of the layer silicates species distribution the primary contact zone structure at Wiry has been proposed (JELITTO & *al.* 1993). SANFORD (1982) suggested that the titanite occurrence could be used as a mark of the initial serpentinite-gneiss contact. The present study shows that the brittle tectonics took place during the contact zones development, as evidenced by epitaxial overgrowths of vermiculite (former mica) on chlorite (Text-fig. 7 *and* Pl. 6, Figs 1-3). Thus, in the studied case only the monoclinic amphibole composition (*see* Text-fig. 10) may be used as a rough indicator of the distance from the leucocratic rock/serpentinite primary contact. The amphibole varieties rich in K+Na, Al, and Fe formed immediately to the pegmatoid, whereas tremolite developed in a distant metasomatic zone and/or in an outlying serpentinite.

EVOLUTION OF LAYER SILICATES *VERSUS* GEOLOGICAL EVENTS

Parent phyllosilicates and their evolution. The polytype investigations of trioctahedral micas and their alteration products was successfully applied to determine the parent mineral in the experimental studies (De la Calle & *al.* 1976) as well as in the altered serpentinite-granite contacts at Szklary and Jordanów in Lower Silesia (Wiewióra & Dubińska 1987, Dubińska & Wiewióra 1988), and at Wiry (Jelitto & *al.* 1993).

According to Jelitto & *al.* (1993) the Wiry vermiculite, mica/vermiculite/chlorite, and mica/vermiculite readily regenerated the phlogopite-like structure, suggesting that phlogopite had been their parent mineral. Despite alteration, the samples rich in these minerals usually display well preserved schistosity, hence the major phyllosilicates evolution was proceeded by transformation; although precipitation of some newly formed clay minerals (*e.g.* smectite) is conspicuous. The predecessor for the interstratified chlorite/vermiculite with asymmetric iron distribution is not clear; its ultimate field association with the interstratified mica/vermiculite (±chlorite) or vermiculite implies the genetic link with former phlogopite zone of the pegmatite/serpentinite contact. In the interstratified minerals with preferential iron location in brucite-like sheet, the chlorite-to-vermiculite and chlorite-to-smectite ratios, and the *R*-value seem to be well constrained within an individual contact zone, but it varies in different zones; probably this diversity resulted from disequilibrium reactions (*see* Bird & Helgeson 1980).

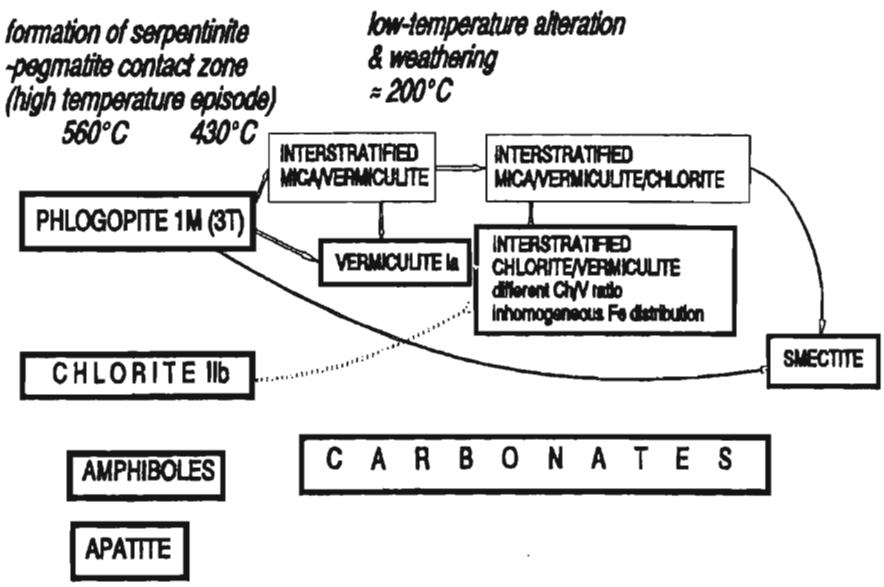

Fig. 28. Schematic diagram of the contact minerals evolution at Wiry (Jelitto & *al.* 1993; *modified*)

Chlorite from the contact rocks either persisted unchanged or yielded "intergradient" minerals with the parent chlorite IIb structure; the "intergradient" minerals could be interpreted as a mixture of interstratified chlorite/vermiculite, chlorite/smectite, and chlorite/smectite/swelling chlorite (JELITTO & *al.* 1993). Thus supposedly, they formed due to the transformation of mica and/or chlorite, as shown at the schematic diagram (Text-fig. 28).

Mobility of iron during mica alteration. Taking into account the expansion of crystal lattice (*c.* 40 vol. %) during the mica → vermiculite transformation, appropriate amounts of elements (Si, Mg, Al, Fe) should simultaneously have been released. Iron behavior during such processes is widely considered (*e.g.* NEWMAN 1967, ROTH & *al.* 1968, FARMER & *al.* 1971, GLIKES & *al.* 1980, Ross & RICH 1974, RANCOURT & *al.* 1993). Composition of phyllosilicates from Wiry evidences constant K/Fe total ratio (*see* Text-fig. 4) during mica → mica/vermiculite → vermiculite transformations, suggesting concomitant iron release. Common admixture of hematite and the interstratified chlorite/vermiculite with preferential iron location in brucite-like sheet probably are the minerals that included the mobilised iron.

Layer silicates from Wiry contact zones *versus* other similar occurrences of Lower Silesia. The mineral assemblages from Wiry (mica, mixed-layer mica/vermiculite, vermiculite, *etc.*) seem to represent a typical early stage of the trioctahedral micas low-temperature alteration (*e.g.* LVOVA & DYAKONOV 1973, BANFIELD & EGGLETON 1988). Phlogopite-derived vermiculite-rich contact schists were reported at Jordanów, in eastern part of the Jordanów-Gogołów serpentinite massif (DUBIŃSKA & WIEWIÓRA 1988, DUBIŃSKA & SZAFRANEK 1990). Highly evolved and nickel-rich products of similar alterations were found in other localities of Lower Silesia, *e.g.* at Szklary as weathered contact granite/ultrabasic rocks (DUBIŃSKA 1982, DUBIŃSKA 1984, WIEWIÓRA & DUBIŃSKA 1987). Exceptionally rich in nickiel corrensite and corrensite-like minerals from Szklary show inhomogeneous nickel distribution (WIEWIÓRA & SZPILA 1975; WIEWIÓRA & ANULEWICZ 1976; DUBIŃSKA 1984; DUBIŃSKA & JELITTO 1992; DUBIŃSKA & SAKHAROV, *unpublished data* 1992), and are similar to the interstratified minerals found in fine-grained fractions of the Wiry samples.

Even relatively altered rocks from the Wiry contact zones are nickel-poor and an increase of Ni/Mg ratio neither in bulk rock nor in mineral compositions were found. Nickel can be mobilized both during hydrothermal alteration (*cf. e.g.* PETRENKO & *al.* 1974, DUCLOUX & *al.* 1993) and chemical weathering of ultrabasic rocks (*e.g.* CHÉTELAT 1947; BASSET 1980; DUCLOUX 1981; NAHON & COLIN 1982; NAHON & *al.* 1982a,b; FONTANAUD & MEUNIER 1983; COLIN &*al.* 1985). Genetic interpretation of Ni-enrichment in altered contact zones at Szklary was ambiguous (DUBIŃSKA 1982).

Consequently, new data are an evidence, that at Szklary massif the highly altered contact zones analogous to these from Wiry, were a structural and

geochemical trap for nickel released from ultramafic rocks during the Tertiary supracrustal weathering.

Acknowledgements

This study has been financed by the National Committee of Scientific Research (*KBN*; Grant No. 6 6309 91 02). The authors express their sincere appreciation to Mr. G. KAPROŃ, Dr. P. DZIERŻANOWSKI, E. FILA M.Sc., H. MUSIAŁOWICZ-KALINOWSKA, E. STARNAWSKA M.Sc., and Dr. P. ZAWIDZKI for technical assistance. Prof. Dr. A. WIEWIÓRA provided an access to X-ray facilities and helpful discussions. Some of the microprobe determinations were performed at the University of Tübingen, Germany, due to kindness of Prof. Dr. P. METZ and technical help of D. MANGLIERS, what is graciously acknowledged. Many of the presented ideas were developed through stimulating discussions with P. BYLINA M.Sc., to whom the authors' appreciation is extended.

Institute of Geochemistry, Mineralogy and Petrography
of the University of Warsaw,
Al. Żwirki i Wigury 93,
02-089 Warsaw, Poland

REFERENCES

BAILEY, S.W. 1982. Nomenclature for regular interstratifications. *A report of the AIPEA Nomenclature Committee, Supplement to AIPEA Newsletters*, **18**, pp. 1-12. Bloomington, Indiana.

— 1984. Structures of layer silicates. *In*: G.W. BRINDLEY & G. BROWN (*Eds*), Crystal structures of clay minerals and their X-ray identification. *Mineralogical Society Monograph*, **5**, pp. 1-124. London.

BANFIELD, J.F. & EGGLETON, R.A. 1988. Transmission electron microscope study of biotite weathering. *Clays & Clay Miner.*, **36** (1), 47-60. Lawrence, Kansas.

BASSET, W.A. 1963. The geology of vermiculite occurrences. *Clays & Clay Miner.*, **12**, 61-69. San Francisco.

BEAUFORT, D. 1987. Interstratified chlorite/smectite ("metamorphic vermiculite") in the Upper Precambrian greywackes of Rouez, Sarthe, France. *In*: L.G. SCHULTZ, H. VAN OLPHEN & F.A. MUMPTON (*Eds*), *Proc. Int. Clay Conf. Denver 1985*, pp. 59-65. *The Clay Min. Soc.*; Bloomington, Indiana.

— & MEUNIER, A. 1994. Saponite, corrensite and chloride-saponite mixed-layer in the Sancerre-Couy deep drill-hole (France). *Clay Miner.*, **29**, 47-61. Cambridge.

BESSET, F. 1980. Localisations et répartitions succesives du nickel au cours de l'altération latéritique des péridotites de Nouvelle-Calédonie. *Mém. Centre d'Études Rech. Géol. Hydrogéol.*, Université des Sciences et Techniques du Languedoc (Montpellier II), CERGA, **15**, pp. 1-129. Montpellier.

BETTISON-VARGA, L., MACINNON, I.D.R. & SCHIFFMAN, P. 1991. Integrated TEM, XRD and electron microprobe investigation of mixed-layer chlorite-smectite from the Point Sal Ophiolite, California, *J. Metamorph. Geol.*, **9**, 697-710. Belfast.

BIRD, D.K. & HELGESON, H.C. 1980. Chemical interaction of aqueous solutions with epidote-feldspar mineral assemblages in geologic systems. 1. Thermodynamic analysis of phase relations in the system CaO-FeO-Fe_2O_3-Al_2O_3-H_2O-CO_2. *Amer. J. Sci.*, **280**, 907-941. New Haven, Connecticut.

BODNAR, R.J. 1993. Revised equation and table determining the freezing point depression of H_2O-NaCl solutions. *Geochim. Cosmochim. Acta*, **57**, 683-684. Oxford.

BUURMAN, P., MEIJER, E.L. & VAN WIJCK, J.H. 1988. Weathering of chlorite and vermiculite in ultramafic rocks of Cabo Ortegal, Northwestern Spain. *Clays & Clay Miner.*, **36**, 263-269. Lawrence, Kansas.

CALLE, C. DE LA, DUBERMAT, J., SUQUET, H., PEZERAT, H., GAULTIER, J. & MAMY J. 1976. Crystal structure of two-layer Mg-vermiculites and Na-, Ca-vermiculites. *Proc. Internatl. Conf. 1975*, Mexico City, pp. 201-209. *Applied Publ. LTD*; Wilmette.

— & SUQUET, H. 1988. Vermiculite. *In*: S.W. BAILEY (*Ed.*), Hydrous phyllosilicates (exclusive of micas), *Reviews in Mineralogy*, **19**, pp. 455-492. *Mineralogical Society of America*; Washington.

CHÉTELAT, E. DE. 1947. La genèse et l'évolution des gisements de nickel de la Nouvelle-Calédonie. *Bull. Soc. Géol. France, Série 5*, **17**, 105-160. Paris.

COLIN, F., NOACK, Y., TRESCAZES, J.-J. & NAHON, D. 1985. L'altération latéritiques debutante des pyroxenites de Jacuba, Niquelandia, Brésil. *Clay Miner.*, **20**, 93-113. Cambridge.

COLLINS, D.R., FITCH, A.N. & CATLOW, R.A. 1992. Dehydration of vermiculites and montmorillonites: a time-resolved powder neutron diffraction study. *J. Mater. Chem.*, **2** (8), 865-873.

CRAWFORD, M.L. 1981. Phase equilibria in aqueous fluid inclusions. *In*: *Short course in fluid inclusions: application to petrology*, pp. 75-100. *Min. Assoc. Can.*; Calgary.

DRITS, V.A. & SAKHAROV, B.A. 1976. X-ray structural analysis of mixed-layer minerals. *Trans. Acad. Sci. U.S.S.R.*, **295**, pp. 1-252. [*In Russian*]. *Publ. House Nauka*; Moscow.

— & KOSSOWSKAYA, A.G. 1990. Clay minerals: smectites, mixed-layer silicates. *Trans. Acad. Sci. U.S.S.R.*, **466**, pp. 1-214. [*In Russian*]. *Publ. House Nauka*; Moscow.

DUBIŃSKA, E. 1982. Nickel-bearing minerals with chlorite-vermiculite intermediate structure from Szklary near Ząbkowice Śląskie (Lower Silesia). *Arch. Miner.*, **38** (1), 27-51. Warszawa.

— 1984. Interstratified minerals with chlorite layers from Szklary near Ząbkowice Śląskie (Lower Silesia). *Arch. Miner.*, **39** (2), 5-23. Warszawa.

— & JELITTO, J. 1992. A simple method of three component interstratified mineral identification. *Ber. Deutsch. Miner. Ges.*, **1**, p. 64. Stuttgart.

— & SZAFRANEK, D. 1990. On the origin of layer silicates from Jordanów (Lower Silesia, Poland). *Arch. Miner.*, **46** (1/2), 19-36. Warszawa.

— & WIEWIÓRA, A. 1988. Layer silicates in the contact zone between granite and serpentinite, Jordanów, Lower Silesia, Poland. *Clay Miner.*, **23**, 459-470. Cambridge.

DUCLOUX, J. 1981. Nickeliferous phyllosilicate as a weathering product of ultramafic rocks. *An International Symposium of Metallogeny of Mafic and Ultramafic Complexes: The Eastern Mediterranean — Western Asia Area, and its Comparison with similar Metallogenic Environments in the World*, **2**, 9-11. Athens.

—, BOUKILI, H., DECAREAU, A., PETIT, S., PERRUCHOT, A. & PRADEL P. 1993. Un gîte hydrothermal de garniérites: l'exemple du Bou Azzer, Maroc. *Eur. J. Miner.*, **5**, 1205-1215. Stuttgart.

FARMER, V.C., RUSSELL, J.L., MCHARDY, W.J., NEWMAN, A.C.D., AHLRICH, J.L. & RIMSAITE, J.Y.H. 1971. Evidence for loss of protons and octahedral iron from oxidized biotites and vermiculites. *Miner. Mag.*, **38** (294), 121-137. London.

FERSMAN, A.E. 1953. Applied geochemistry. *In*: *Selected works*, **2**, 403-758. *Acad. Sci. USSR Publ. House*; Moscow.

FONTANAUD, A. & MEUNIER, A. 1983. Mineralogical facies of a weathered serpentinized lherzolite from Pyrenées, France. *Clay Miner.*, **18**, 77-88. Cambridge.

GAJEWSKI, Z. 1970. Occurrence and properties of magnesites from the Gogołów-Jordanów serpentinite massif against the geological structure of the area. *Biul. Inst. Geol.*, **240**, 55-142. [*In Polish*]. Warszawa.

GILKES, R.J., SUDDHIPRAKARN, A. & ARMITAGE, T.M. 1980. Scanning electron microscope morphology of deeply weathered granite. *Clays & Clay Miner.*, **28** (1), 29-34. San Francisco.

HAAS, J.L., Jr. 1976a. Physical properties of coexisting phases and thermochemical properties of the H_2O component in boiling NaCl solutions. *Geol. Surv. Bull.*, **1421-A**, pp. A1-A73. Washington, D.C.

— 1976b. Thermodynamic properties of coexisting phases and thermochemical properties of the NaCl component in boiling NaCl solutions. *Geol. Surv. Bull.*, **1421-B**, pp. B1-B71. Washington, D.C.

HALL, D.L., STERNER, S.M. & BODNAR, R.J. 1988. Freezing point depression of NaCl-KCl-H_2O solutions. *Econ. Geol.*, **83**, 197-202. Lancaster, Pennsylvania.

HAMMARSTROM, J.M. & ZEN, E-AN. 1986. Aluminium in hornblende: an empirical igneous geobarometer. *Amer. Miner.*, **71**, 1297-1313. Washington, D.C.

HARAŃCZYK, C. & PROCHAZKA, K. 1974. Hydrated magnesium-nickel silicates from Wiry (Lower Silesia). *Pr. Muz. Ziemi.*, **22**, 2-62. Warszawa.

— & WALA, A. 1970. Endogenic mineralization in ultrabasic massifs of northern foreland of central Sudetes Mts. *Przegl. Geol.*, **18** (6), 274-282. Warszawa.

HOLLISTER, L.S., GRISSOM, G.C., PETERS, E.K., STOWELL, H.H. & SISSON, V.B. 1987. Confirmation of the empirical correlation of Al in hornblende with pressure of solidification of calc-alkaline plutons. *Amer. Miner.*, **72**, 231-239. Lawrence, Kansas.

INOUE, A. & UTADA, M. 1991. Smectite to chlorite transformation in thermally metamorphosed volcanoclastic rocks in the Kamikita Area, northern Honshu, Japan. *Amer. Miner.*, **76**, 628-649. Lawrence, Kansas.

JANECZEK, J. & SACHANBIŃSKI, M. 1995. New data on hybrid pegmatites in serpentinites of the Wiry Magnesite Mine (Lower Silesia, SW Poland). *Przegl. Geol.*, **43** (9), 777-782. Warszawa.

JĘDRYSEK, M.O. & HAŁAS, S. 1990. The origin of magnesite deposits from the Polish Foresudetic Block ophiolites: Preliminary $\delta^{13}C$ and $\delta^{18}O$ investigations. *Terra Nova*, **2**, 154-159. Oxford.

JELITTO, J., DUBIŃSKA, E. & WIEWIÓRA, A. 1991. Evolution of trioctahedral layer silicates from contact serpentinite-pegmatite (Wiry, Lower Silesia, Poland). *In*: M. STÖRR, K.-H. HENNIG

& P. ADOLPHI (*Eds*), *Proc. 7th EUROCLAY Conf. Dresden 1991.*, II, p. 547-552. *Ernst-Moritz-Arndt Universität*; Greifswald.

— , — , — & BYLINA, P. 1993. Layer silicates from serpentinite-pegmatite contact (Wiry, Lower Silesia Poland). *Clays & Clay Miner.*, **41** (6), 693-701. Lawrence, Kansas.

JOHNSON, M.C. & RUTHERFORD, M.J. 1989. Experimental calibration of the aluminium-in-hornblende geobarometer with application to Long Valley Caldera (California) volcanic rocks. *Geology*, **17**, 837-841. Boulder.

KARWOWSKI, Ł., KOZŁOWSKI, A. & ROEDDER, E. 1979. Gas-liquid inclusions in minerals of zinc and lead ores from the Silesia-Cracow region. *Prace I. G.*, **95**, 87-96. Warszawa.

KIMPE, C.R. DE, MILES, N., KODAMA, H. & DEJOU, J. 1987. Alteration of phlogopite to corrensite at Sharbot Lake, Ontario. *Clays & Clay Miner.*, **35**, 150-158. Lawrence, Kansas.

KOSZELA, S. 1984. Granitic pegmatite in serpentinite. *In*: A. MAJEROWICZ (*Ed.*), Mineralogy and tectonics of Strzegom-Sobótka granitoid massif, pp. 112-118. [*In Polish*]. *Univ. Wrocl. Publ. House*; Wrocław.

KOZŁOWSKI, A. 1978. Pneumatolytic and hydrothermal activity in the Karkonosze-Izera block. *Acta Geol. Polon.*, **28** (2), 171-222. Warszawa.

— 1984. Calcium-rich inclusion solutions in fluorite from the Strzegom pegmatites, Lower Silesia. *Acta Geol. Polon.*, **34** (1/2), 132-138.

— 1994. Defected quartz crystals, fluid inclusions and wallrock joint fractures in Strzegom pegmatites. *Fifth Biennial Pan-American Conf. on Res. on Fluid Inclusions Abstracts*, pp. 50-51. Cuernavaca.

— & SACHANBIŃSKI, M. 1984. Remarks on genesis of Polish chrysoprase as indicated by inclusion studies. *Fluid Incl. Res.-Proc. of COFFI*, **17**, 402-404. *Univ. Mich. Press*; Ann Arbor, Michigan.

KURAL, S. & MORAWSKI, T. 1968. Strzegom-Sobótka granitic massif. *BIUL. Inst. Geol.*, **227** (17), 1-57. [*In Polish*]. Warsaw.

LVOVA, I.A. & DYAKONOV, Y.C. 1973. Geological and mineralogical criteria of estimation of vermiculite raw material occurrences related to ultrabasic rocks. Non-metalic raw materials in ultramafic rocks, p. 207-210. [*In Russian*]. *Publ. House Nauka*; Moscow.

MAJEROWICZ, A. 1972. Strzegom granitic massif. A petrological study. *Geol. Sudetica*, **6**, 7-96. Wrocław.

— 1979. The mountain group of Ślęża and recent petrological problems of the ophiolites. *In*: *Selected stratigraphical, petrographical and tectonic problems of the eastern border of the gneisses of Sowie Góry Mts. and Kłodzko metamorphic structure. Materials of the Field Conf. Nowa Ruda*, pp. 9-34. [*In Polish*]. *Univ. Wrocław. Publ. House*; Wrocław.

— 1981. Rock series of the Ślęża Mt. group in the light of petrologic studies of ophiolitic complexes. *Ophiolites and initialites of the northern border of the Bohemian Massif*, **2**, pp. 172-193. Potsdam — Freiberg.

— & PIN, C. 1994. The main petrological problems of the Mt. Ślęża ophiolite complex, Sudetes, Poland. *Zbl. Geol. Paläont.*, Teil 1 (9/10), 989-1018. Stuttgart.

MARSHALL, B. & MANCINI, F. 1994. Major- and minor-element mobilization, with implications for Ni-Cu-Fe-sulphide remobilization, during retrograde metasomatism at the Vammala Mine, southwest Finland. *Chem. Geol.*, **116**, 203-227. Amsterdam.

MATTHES, S. & OLESCH, M. 1986. Polymetamorphic-metasomatic blackwall rocks of the Falkenberg granite contact aureole near Erbensdorf, Oberpfalz, Bavaria. *Neues Jb. Miner. Abh.*, **153** (3), 325-362. Stuttgart.

MERING, S. 1949. X-ray diffraction in disordered layer structures. *Acta Cryst.*, **2**, 371-377.

MUSIAŁ, W. 1992. DRONEK-2. Computerized interface for GUR-5 goniometer. *Unpubl. manuscript*, pp. 1-9. Kraków.

NAGASAWA, K., BROWN, G. & NEWMAN, A.C.D. 1974. Artifical alteration of biotite into a 14 Å-layer silicate with hydroxy-aluminium interlayers. *Clays & Clay Miner.*, **22**, 241-252. San Francisco.

NAHON, D.B. & COLIN, F. 1982. Chemical weathering of orthopyroxenes under lateric conditions. *Amer. J. Sci.*, **282**, 1232-1243. New Haven, Connecticut.

— , — & TARDY, Y. 1982a. Formation and distribution of Mg, Fe, Mn-smectites in the first stages of the lateritic weathering of forsterite and tephorite. *Clay Minerals*, **17**, 339-348. Cambridge.

NAHON, D., PAQUET, H. & DELVIGNE, J. 1982b. Lateritic weathering of ultramafic rocks and the concentration of nickel in the western Ivory Coast. *Econ. Geol.*, **77**, 1159-1175. Lancaster, Pennsylvania.

NARĘBSKI, W. 1994. Lower to Upper Paleozoic tectomagmatic evolution of NE part of the Bohemian Massif. *Zbl. Geol. Paläont.*, Teil 1 (9/10), 961-972. Stuttgart.

— & MAJEROWICZ, A. 1985. Ophiolites of the Sowie Góry Mts. framework and Lower Paleozoic initialites of the Polish Sudetes. *In*: N.I. DOBRETSOV (*Ed.*), Riphean-Lower Paleozoic ophiolites of north Eurasia, pp. 86-105. [*In Russian*]. *Publ. House Nauka*; Novosibirsk.

— , WAJSPRYCH, B. & BAKUN-CZUBAROW, N. 1982. On the nature, origin and geotectonic significance of ophiolites and related rock suites in the Polish part of Sudetes. *Ofioliti*, **2/3**, 407-428. Milano.

NEWMAN, A.C.D. 1967. Changes in phlogopites during their artifical alteration. *Clay Minerals*, **7**, 215-227. Cambridge.

NISHIYAMA, T., OINUMA, K. & SATO, M. 1979. An interstratified chlorite-vermiculite in weathered red shale near Tiyoma, Japan. *In*: M.M. MORTLAND & V.C. FARMER (*Eds*), International Clay Conference 1978 held in Oxford, *Developments in Sedimentology*, **27**, pp. 85-94. *Elsevier*; Amsterdam.

NIŚKIEWICZ, J. 1970. Characteristics of serpentinization of ultrabasic rocks from Lower Silesia. *Przegl. Geol.*, **18** (6), 271-274. Warszawa.

NOACK, Y. & COLIN, F. 1986. Chlorites and chloritic mixed-layer minerals in profiles on ultrabasic rocks from Moyango (Ivory Coast) and Angiquino (Brazil). *Clay Miner.*, **21**, 171-182. Cambridge.

NOWAKOWSKI, A. & KOZŁOWSKI, A. 1984. Genesis and crystallization conditions of albite in pegmatites of the Karkonosze and Strzegom granites. *Arch. Miner.*, **39**, 5-15. Warszawa.

OLIVER, G.J.H., CORFU, F. & KROGH, T.E. 1993. U-Pb ages from SW Poland: evidence for a Caledonian suture zone between Baltica and Gondwana. *J. Geol. Soc. London*, **150** (2), 355-369. London.

PENDIAS, H. & WALENCZAK, Z. 1956. Signs of mineralization in the north-western part of Strzegom massif, Lower Silesia. *Biul. Inst. Geol.*, **112**, 209-240. Warszawa.

PETRENKO, G.V., ARUTYUNYAN, L.A., ZHANGUROV, A.A., MITYUNIN, Y.K. & PREDOVSKIY, A.A. 1974. On the possibility of hydrothermal nickel leaching from olivinites. *Geokhimya*, **8**, 1185-1191. [*In Russian*]. Moscow.

PIN, C., MAJEROWICZ, A. & WOJCIECHOWSKA, I. 1988. Upper Paleozoic oceanic crust in the Polish Sudetes: Nd-Sr isotope and trace element evidence. *Lithos*, **21**, 195-209. Amsterdam.

— , PUZIEWICZ, J. & DUTHOU, J.L. 1989. Ages and origins of a composite granitic massif in the Variscan belt: a Rb-Sr study of the Strzegom Massif, W. Sudetes (Poland). *N. Jb. Miner., Abh.*, **160**, 71-82. Stuttgart.

POTTER, R.W.H. & BROWN, D.L. 1977. The volumetric properties of aqueous sodium chloride solutions from 0° to 500°C at pressures up 2000 bars based on regression of available data in the literature. *Geol. Surv. Bull.*, **1421-C**, pp. C1-C36. Washington, D.C.

— , CLYNNE, M.A. & BROWN, D.L. 1978. Freezing point depression of aqueous sodium chloride solutions. *Econ. Geol.*, **73**, 284-285. Lancaster, Pennsylvania.

PROUST, D., EYMERY, J.P. & BEAUFORT, D. 1986. Supergene vermiculitization of a magnesian chlorite: iron and magnesium removal processes. *Clays & Clay Miner.*, **34**, 572-580. Lawrence, Kansas.

RANCOURT, D.G., TUME, P. & LALONDE, A.E. 1993. Kinetics of the $(Fe^{2+}+OH^{-})_{mica}$-$(Fe^{3+}+O^{2-})_{mica}+H$. Oxidation reaction in bulk single-crystal biotite studied by Mössbauer spectroscopy. *Phys. Chem. Minerals*, **20**, 276-284. Berlin.

REYNOLDS, R.C., Jr. 1980. Interstratified clay minerals and their X-ray identification. *Mineralogical Society Monographs*, **5**, 249-303. London.

— 1985. NEWMOD, a computer program for the calculation of one-dimensional diffraction patterns of mixed-layer clays. *Publ. by author*; Hanover, New Hampshire.

— 1988. Mixed-layer chlorite minerals. *In*: S.W. BAILEY (*Ed.*), Hydrous phyllosilicates (exclusive of micas), *Reviews in Mineralogy*, **19**, 601-629. *Min. Soc. Amer.*; Washington, D.C.

RICH, C.I. 1968. Hydroxy interlayers in expansible layer silicates: *Clays & Clay Minerals*, **16**, 15-30. San Francisco, California.

ROBINSON D., BEVINS R.E. & ROWBOTHAM G. 1993. The characterization of mafic phyllosilicates in low-grade metabasalts from eastern north Greenland. *Amer. Miner.*, **78**, 377-399. Lawrence, Kansas.

ROEDDER, E. 1984. Fluid inclusions. *Reviews in Mineralogy*, **12**, p. 480. *Min. Soc. Amer.*; Blacksburg, Virginia.

ROSS, G.I. & RICH, C.I. 1974. Effect of oxidation and reduction on potassium exchange of biotite. *Clays & Clay Miner.*, **22** (4), 355-360. San Francisco, California.

ROTH, C.B., JACKSON, M.L., LOTSE, E.G. & SYERS, J.K. 1968. Ferrous-ferric ratio and CEC changes of deferration of weathered micaceous vermiculite. *Israel J. Chem.*, **6**, 261-273. Jerusalem.

SACHANBIŃSKI, M. 1993. Złoże talku i wermikulitu "Wiry" w ultramafitach ofiolitu Ślęży (Dolny Śląsk). *Acta Univ. Wratisl.*, **1412** (*Pr. Geol.-Miner.* **33**), pp. 63-117. Wrocław.

SANFORD, R.F. 1982. Growth of ultramafic reaction zones in greenschist to amphibolite facies metamorphism. *Amer. J. Sci.*, **282**, 543-616. New Haven, Connecticut.

SCHIFFMAN, P. & FRIDLEIFSSON, G.O. 1991. The smectite-chlorite transition in drillhole NJ-15, Nesjavellir geothermal field: XRD, BSE and electron microprobe investigations. *J. Metamorph. Geology*, **9**, 679-696. Belfast.

SHAU, Y.-H., PEACOR, D.R. & ESSENE, E.J. 1990. Corrensite and mixed-layer chlorite/corrensite in metabasalt from northern Taiwan: TEM/AEM, EMPA, XRD, and optical studies. *Contrib. Miner. Petrol.*, **105**, 123-142. Würzburg.

TEISSEYRE, H., SMULIKOWSKI, K. & OBERC, J. 1957. Sudetes. Pre-Tertiary deposits. *Regional Geology of Poland*, **3** (1), pp. 1-300. [*In Polish*]. *PWN.*; Kraków.

TROMMSDORFF, V. & EVANS, B.W. 1972. Progressive metamorphism of antigorite schist in the Bergell tonalite aureole (Italy). *Amer. J. Sci.*, **272** (5), 423-437. New Haven, Connecticut.

WADA, N., HINES, D.R. & AHRENKIEL, S.P. 1990. X-ray diffraction studies of hydration transitions in Na-vermiculite. *Phys. Rev.*, **41** (18), 12895-12901.

WEISS, Z. & WIEWIÓRA, A. 1986. Polytypism of micas. III. X-ray diffraction identification. *Clays & Clay Miner.*, **34**, 53-68. Lawrence, Kansas.

WICKS, F.J. & O'HANLEY, D.S. 1988. Serpentine minerals: structure and petrology. *In*: S.W. BAILEY (*Ed.*), Hydrous phyllosilicates (exclusive of micas), *Reviews in Mineralogy*, **19**, 91-167. *Mineralogical Society of America*; Washington, D.C.

WIEWIÓRA, A. & ANULEWICZ, A. 1976. The polarity of 2:1 layers in a regularly interstratified Ni-chlorite-saponite from Lower Silesia (Poland). *Bull. Acad. Polon. Sci., Sér. Sci. Terre*, **24** (3/4), 163-166. Warszawa.

— & DUBIŃSKA, E. 1987. Origin of minerals with intermediate chlorite-vermiculite structure (Szklary, Lower Silesia). *Chem. Geol.*, **60**, 185-197. Amsterdam.

— & SZPILA, K. 1975. Nickel containing regularly interstratified chlorite-saponite from Szklary, Lower Silesia, Poland. *Clays & Clay Miner.*, **23**, 91-96. San Francisco, California.

— & WEISS, Z. 1985. X-ray powder transmission diffractometry determination of mica polytypes: method and application to natural samples. *Clay Miner.*, **20**, 231-248. Cambridge.

ZILBERFARB, A. & NATHAN, Y. 1986. Contact metasomatism in the Dahab Area (Eastern Sinai). *Israel J. Earth Sci.*, **35**, 1-9. Jerusalem.

E. DUBIŃSKA, J. JELITTO i A. KOZŁOWSKI

GENEZA I EWOLUCJA STREF REAKCYJNYCH POMIĘDZY GRANITEM I SERPENTYNITEM W WIRACH

(Streszczenie)

Przedmiotem pracy jest analiza składu i powstawania łupków kontaktowych, rozwiniętych pomiędzy apofizami waryscyjskich granitoidów hybrydalnych a starszymi od nich serpentynitami masywu Jordanów-Gogołów (fig. 1-3 *oraz* pl. 1-6). Łupki te zbudowane są z flogopitu, chlorytu, talku, amfiboli o składzie od tremolitu do pargasytu (tab. 1-3 *oraz* fig. 4-11) i podrzędnego apatytu. Są to pierwotne minerały badanych stref kontaktowych, które powstały pod ciśnieniem $\leqslant$2,6 Kbar i w temperaturach $\leqslant$560°C (fig. 23 *oraz* 26). W miarę spadku temperatury z wyjściowych łyszczyków i chlorytów (fig. 28) rozwijał się urozmaicony zespół krzemianów warstwowych: wermikulit, smektyt, regularnie mieszanopakietowy łyszczyk/wermikulit, zrożnicowane minerały mieszanopakietowe typu chloryt/wermikulit z asymetrycznym rozmieszczeniem żelaza, trójskładnikowy mieszanopakietowy łyszczyk/wermikulit/chloryt, i in. (fig. 13-22).

Strefy kontaktowe rozwijały się kosztem serpentynitu, o czym świadczą ich tekstury i charakterystyka geochemiczna (tab. 4-5 *oraz* fig. 12). Powstanie łyszczków, chlorytu i amfiboli wymagało dopływu K, Na, Ca i Al, uruchamianych (oprócz innych pierwiastków) podczas hybrydyzacji dajek granitoidowych, związanej z ich albityzacją (fig. 24-25 *oraz* 27).

Strefy kontaktowe z Wir wykazują budowę analogiczną do niklonośnych stref złożowych z masywu serpentynitowego Szklar. Mogły one być w masywie Szklar pułapkami geochemicznymi dla niklu, uruchamianego w trakcie wietrzenia ultrabazytów, a następnie wychwytywanego prawdopodobnie przez minerały mieszanopakietowe chloryt/wermikulit z asymetrycznym rozmieszczeniem żelaza.

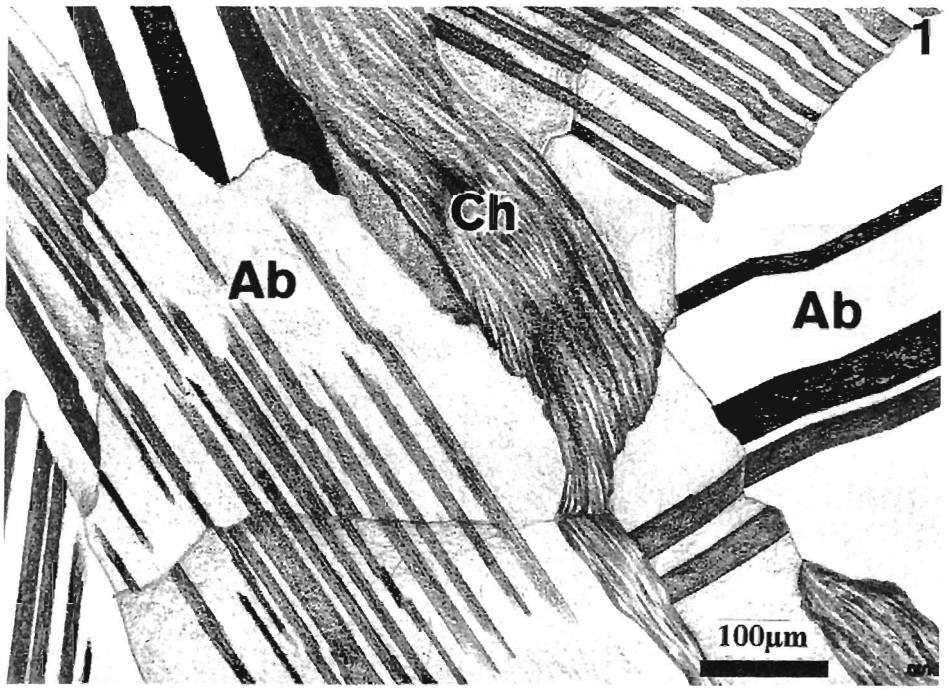

1 – Highly tectonized albite (**Ab**) pegmatoid with the chlorite (**Ch**) contact schist displaced into the pegmatoid fracture; crossed polars, sketch after thin section, sample *Wi106*, kindly submitted by P. BYLINA, M.Sc.

2 – Pseudomorphic serpentinite with hour-glass pseudomorphs after olivine; crossed polars, sample *Wi26s*

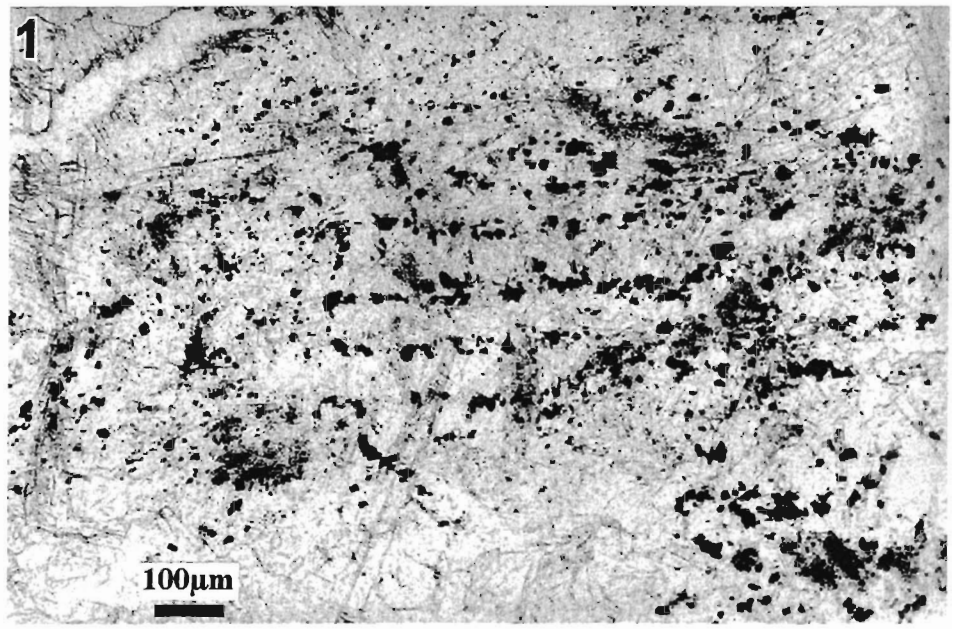

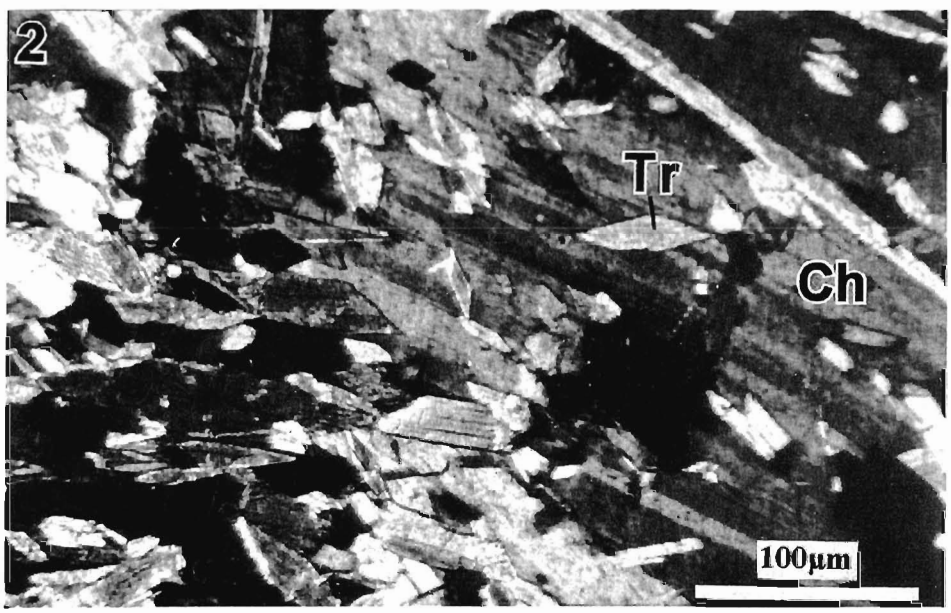

1 – Tremolite-chlorite schist with a pseudomorph after pyroxene, as evidenced by small grains of magnetite arranged in striae parallel to the previous (100) partings of pyroxene; one polar, sample *Wi15C*

2 – Tremolite(**Tr**)–chlorite(**Ch**) schist with random distribution of the amphibole prisms; crossed polars, sample *Wi15C*

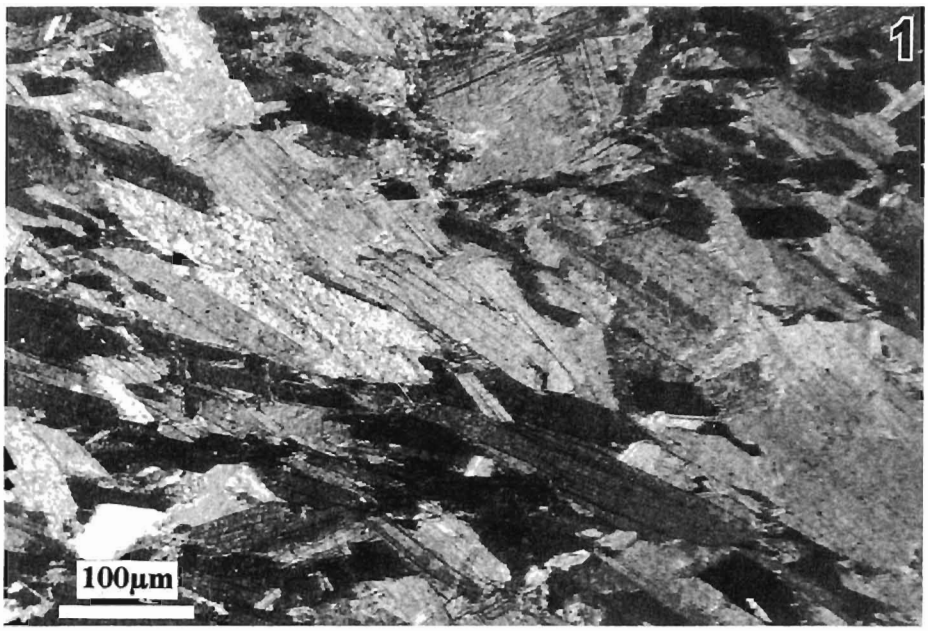

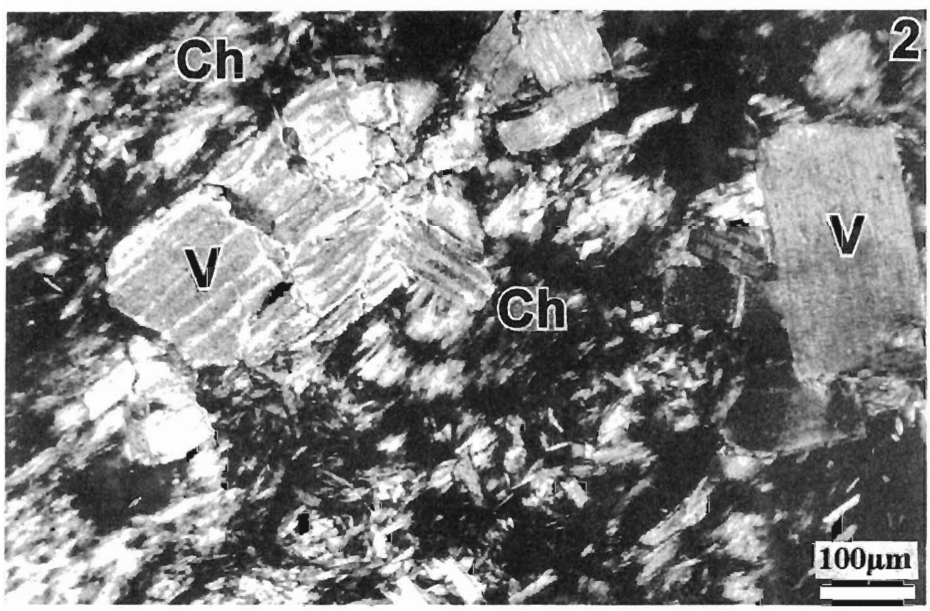

1 – Phlogopite schist; crossed polars, sample *W2*

2 – Vermiculite-like (V) flakes (previous phlogopite) in the tectonized chlorite (Ch) matrix; crossed polars, sample *Wi12B*

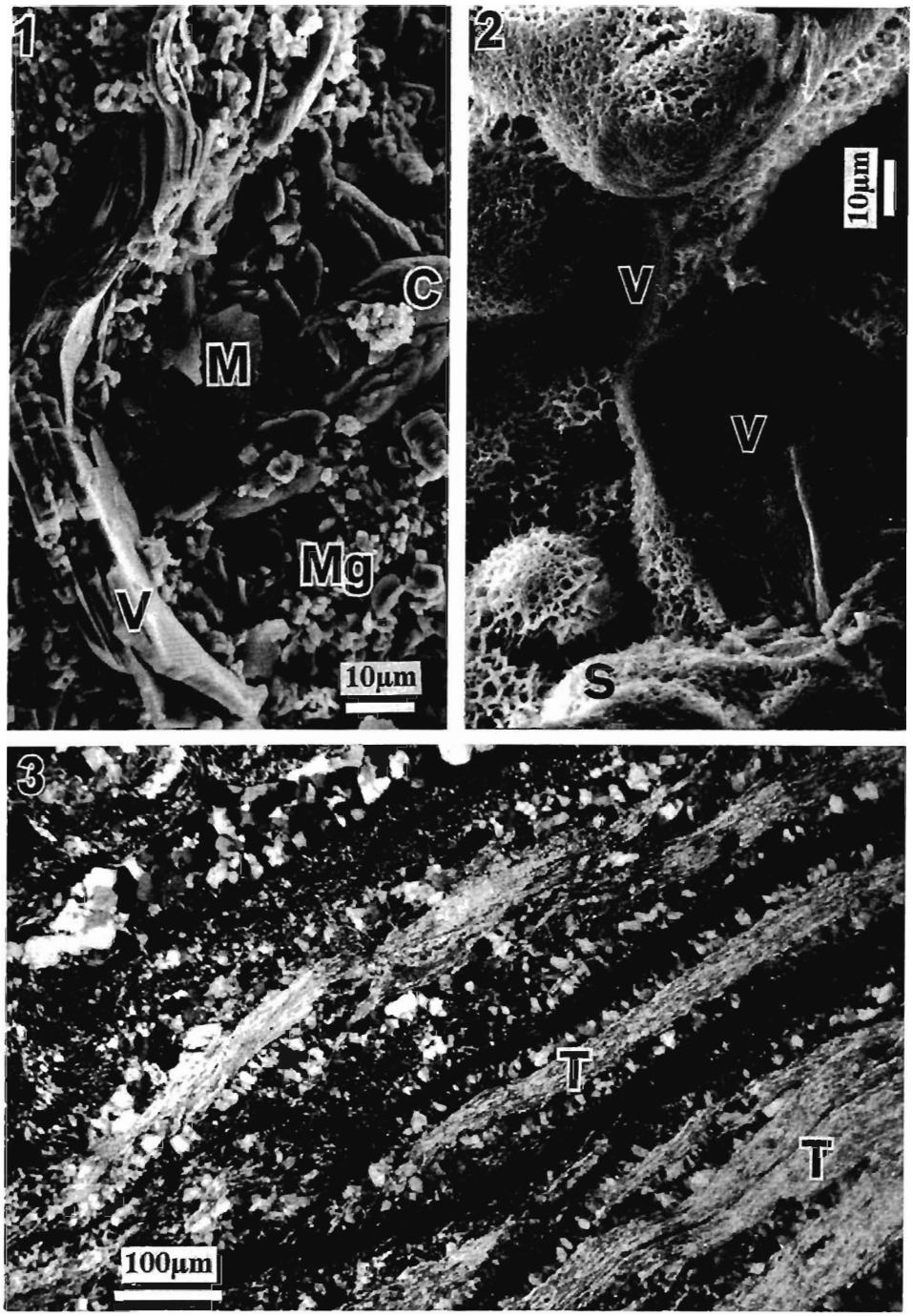

1 – Flat phlogopite (**M**) and bent vermiculite (**V**) flakes surrounded by fine-grained magnesite (**Mg**) and cone-like calcite (**C**) intergrowths; sample *Wi33*, SEM photo taken by Dr. P. ZAWIDZKI

2 – Spongy smectite coatings (**S**) on vermiculite (**V**) flakes; sample *W3* after ultrasonic treatment, SEM photo taken by Dr. P. DZIERŻANOWSKI

3 – Talc (**T**) schist with quartz and chalcedony veinlets; crossed polars, sample *Wi8*

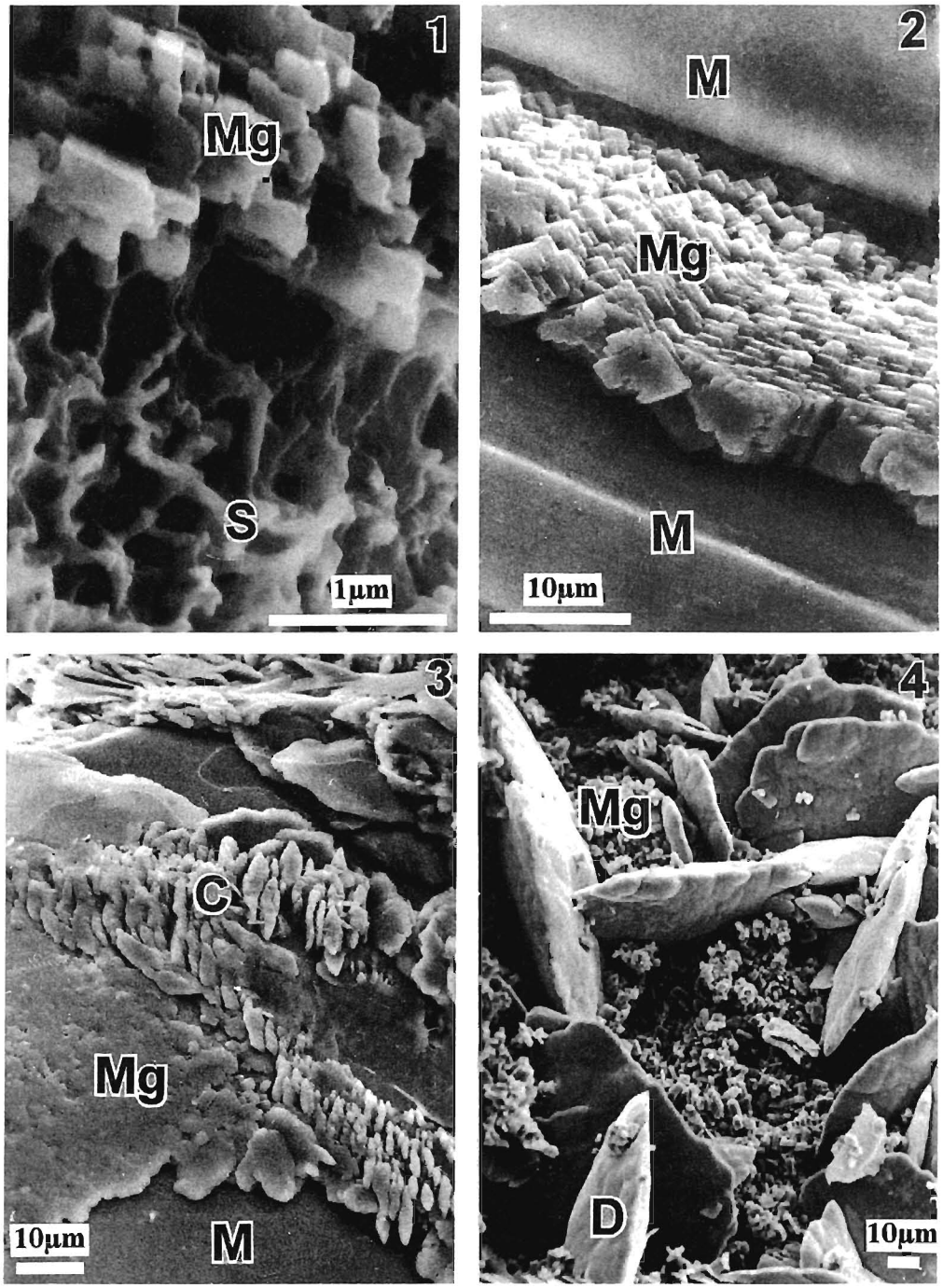

1 – Magnesite (**Mg**) and smectite (**S**) intergrowths; sample *Wi3*, SEM photo taken by Dr. P. DZIERŻANOWSKI

2 – Phlogopite (**M**) flakes with magnesite (**Mg**) rhombohedrons; sample *Wi5D* after ultrasonic treatment, SEM photo taken by Dr. P. DZIERŻANOWSKI

3 – Almond-shaped calcite (**C**) veinlet cutting the fine-grained magnesite (**Mg**) coating on a phlogopite (**M**) flake; sample *Wi5D* after utlrasonic treatment, SEM photo taken by Dr. P. DZIERŻANOWSKI

4 – Flat rhombohedrons of dolomite (**D**) and fine-grained magnesite (**Mg**) intergrowths; sample *Wi33*, SEM photo taken by E. FILA, M.Sc.

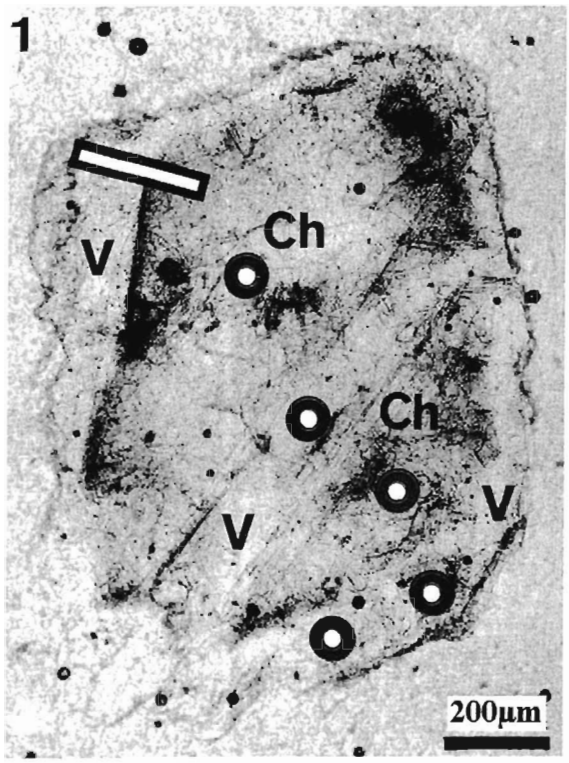

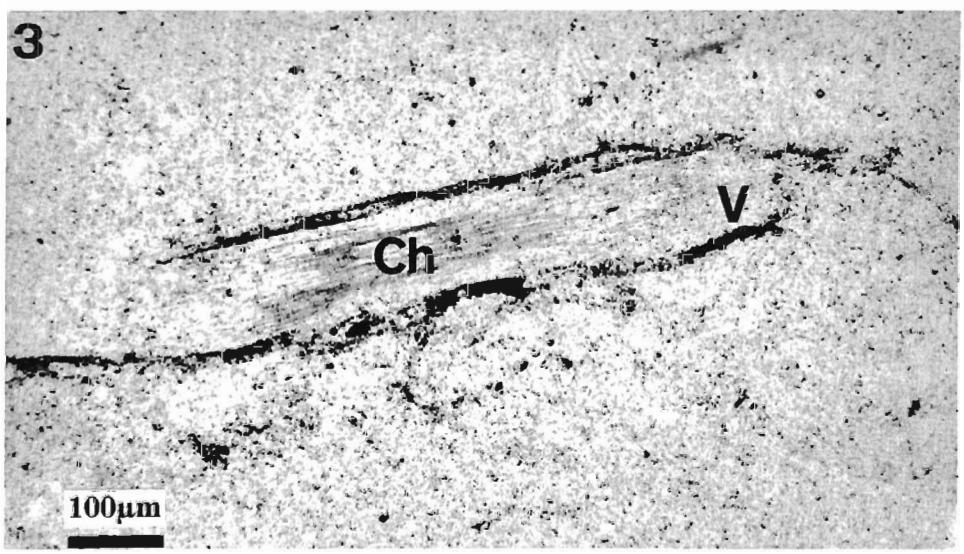

1 – Inhomogeneous (001) flake consisting of the chlorite (**Ch**) core and a vermiculite-like mineral (**V**) rim, mounted in epoxy; analysed points are indicated by circles (*see* Text-fig. 7); one polar, sample *Wi2A*, photo taken by Docent A. Nowakowski

2-3 – Sections ⊥(001) of inhomogeneous flakes consisting of the chlorite (**Ch**) core and a vermiculite-like mineral (**V**) rim; matrix – tectonized vermiculite (previous mica); one polar, sample *Wi2A*, photo taken by Docent A. Nowakowski